Journal of Research and Didactics in Geography (J-READING), 2, 2, Dec., 2013, pp. 115-142
DOI: 10.4458/2379-10

J - READING
JOURNAL OF RESEARCH AND DIDACTICS IN
GEOGRAPHY
homepage: www.j-reading.org

Remote sensing and interdisciplinary approach for studying glaciers

Maurizio Fea[a], Umberto Minora[b], Cristiano Pesaresi[c], Claudio Smiraglia[d]
[a] Italian Geophysics Association, Rome, Italy
[b] Dipartimento di Scienze della Terra "Ardito Desio", University of Milan, Milan, Italy
[c] Dipartimento di Scienze documentarie, linguistico-filologiche e geografiche, Sapienza University of Rome, Rome, Italy
[d] Dipartimento di Scienze della Terra "Ardito Desio", University of Milan, Milan, Italy – Comitato Glaciologico Italiano

Email: claudio.smiraglia@unimi.it

Received: November 2013 – Accepted: December 2013

Abstract

Remote sensing, which provides interesting input and approaches for multidisciplinary research and wide inventories, and which represents a very important tool in the strictly related fields of research and didactics, shows great potentialities in the specific area of the studies of glaciers (extension, balance and variations), glacier morphology and climate changes. In time, remote sensing applications for the analysis of glaciers and climate change have considerably increased, using different methodologies and obtaining significant results. In this paper, after a synthesis of some basic elements, we provide a detailed literary review, which sets out to underline the steps and results achieved and also to stimulate didactical considerations and hypothesis of work. Successively, we resume the main characteristics of specific glaciers, for which the European Space Agency (ESA-ESRIN) has provided images *ad hoc* and for each glacier we propose an interpretative analysis of these images. According to the scheme proposed by Fea et al. (2013), the principal aim is to define research of referral and some interpretative guidelines useful for interdisciplinary frameworks focussed on glaciers, where geography can play the role of collector between different sciences with the support of various geotechnologies.

Keywords: Climate Change, Glaciers, Ice and Snow, Interdisciplinary Study, Remote Sensing, Satellite and Aerial Images

1. Introduction

The modern knowledge of the planet Earth describes it as an integrated system of six basic components, namely atmosphere, cryosphere, hydrosphere, geosphere, biosphere and anthroposphere, each of them in a permanent and complex interaction with all the others. The evolution of the Earth is characterised primarily by this interactivity, even if in the medium- and

long-term an important role is played by external forces, such as solar wind and cosmic rays, and sometimes by sudden interplanetary events, for instance by the impact of a celestial body.

Nowadays, major scientific challenges are concerned with the apparent acceleration of the evolution of the Earth's climate, the increased occurrence of extreme meteorological events and atmospheric global warming. The real concern comes, in particular, from the actual impact that is caused to the above-mentioned natural evolution by the parallel exponential increase of the world population and human activities.

Specifically, two terms have become very popular: *climate change* and *global warming*, implying in reality with them the impact on natural phenomena (climate variability and atmospheric greenhouse effect) of human activities. Therefore, climate change and global warming are now first priority targets (among others, of course) for scientific research and world-wide operational observing systems. General and specific phenomena and parameters have been identified for an effective monitoring through measurements and observations at all scales and with all means, from ground devices to airplane and satellite instruments.

In the above context, the accurate monitoring of the cryosphere plays a very important role, as ice in all its forms, such as sea-ice, permafrost, glaciers, icebergs, snow cover and so on, has a fundamental role in the variability of key physical and chemical parameters, like for instance temperature, albedo, sublimation, pollution. Therefore, glaciers are very important scientific and operational indicators, as will be shown and demonstrated in the next chapters.

One last consideration concerns remote sensing, that is to say methodology, procedures and tools for observing a target without getting into physical contact with it. It uses devices (sensors) that measure the electromagnetic energy irradiated by the observed targets in different parts (spectral bands) of the electromagnetic (e.m.) spectrum, defined by their related wavelengths. The most common bands used to observe the Earth's surface are the Visible (VIS, which contains all the colours of a rainbow), Near-, Medium- and Far Infrared (NIR, MIR and FIR), the Thermal Infrared (TIR) and the Microwaves (MW).

The energy measured in each spectral band carries a different type of information about the observed target: for example, in the Visible the physical input is the fraction of sunlight (albedo) reflected by the target surface towards the sensor. Simultaneous use of different VIS bands provides information that is very useful to "recognise" the observed target and, therefore, to "classify" it through a *multispectral* observation. Each spectral band used by an observing instrument has a number assigned, specific to that instrument; the same band with a different instrument could have a different number. The data are then visualised on a screen by inserting the values measured in a spectral band in one of the three colour channels (Red, Green and Blue) that drive the screen; the visualisation model is then identified by specifying RGB and the band numbers used to visualise the band values: for example, RGB 321 indicates that the data acquired by the sensor in the spectral band No. 3 of the used instrument are shown in Red colour tones on the screen.

Visualisation in *natural* (or *true*) *colours* means inserting into the RGB channels of the screen respectively the values measured by the sensor through the spectral bands of the corresponding red, green and blue colours of the rainbow in the Visible bands. Any other combination would provide a *false colour* image on the screen. Natural colour images provide a "human" view of the scene; false colours are very much used to help the interpretation of the data or to quickly identify a specific target (thematic images).

This paper, conducted on the basis of the scheme proposed by Fea et al. (2013), focusses the attention on specific elements that would help to better understand the potentialities of remote sensing in the double and strictly related fields of research and didactics, resuming the methods and results of many studies carried out on different glaciers and examining various glaciers under a geographic, glaciological and geomatic point of view.

2. Remote sensing for the study of mountain glaciers. A literary review and some didactical considerations

International literature has shown many interesting and useful functions and applications regarding remote sensing for the study of glaciers (extension, balance and variations) and glacier morphology, also providing input for the analysis of climate change. In fact, there is a very large amount of research which has focussed the attention on different glaciers, providing important estimates regarding the dimensions and variations recorded over a number of years or decades. For example, the glaciers of the Himalayas and the Alps are precious sources of information and data because they have been analysed considering many aspects and points of view. In other cases, remote sensing has been used as a support for the assessment of hazards from glacier lake outbursts and for the origination of potential ice avalanches and debris flows and also for the evaluation of permafrost-related hazards in high mountains (Huggel et al., 2002; Kääb et al., 2005; Frey et al., 2010).

In order to collect a set of images that are explanatory and of considerable use both in research and didactics, it is very important to have images obtained over a period with a reduced blanket of snow and without cloud cover; similarly, in terms of evolution analysis, it would be recommended to make comparisons among images taken in the same month in different years so as to permit maximum comparability.

For some decades now many papers have underlined the potential added value of remote sensing for the study of glaciers, highlighting particular aspects and providing relevant contributions for different kinds of analysis, and in the last ten years an intense proliferation of studies has been recorded, stimulating the need to define synthetic frameworks of knowledge and results.

As affirmed by Berthier et al. in 2004, mountain glaciers can be considered a reliable indicator of climate change and remote sensing can provide "a suitable way to increase the number of monitored glaciers, especially in remote areas". Focussing the attention on the Mer de Glace, the largest glacier in the French Alps, as "test area", the approach used has adapted "the geodetic method to satellite images. The first step calculates the DEMs. Some adjustments and corrections are needed to reduce the biases between the DEMs. The mean thickness change is then extracted for each altitude interval on the glacier" (p. 1). Considering two time intervals (1994-2000 and 2000-2003), the study has made it possible to "show a rapid thinning of the Mer de Glace during the last 10 years below 2500 m" (p. 4).

A couple of years later, Bolch and Kamp stated that: "Glaciers are sensitive climate indicators and thus subject to monitoring of environmental and climate changes. Remote sensing techniques are often the only way to analyze glaciers in remote mountains and to monitor a large number of glaciers at the same time" (2006, p. 37). Their study has shown "the capability of accurate glacier mapping using multispectral data, digital elevation models (DEMs), and morphometric analysis for the Bernina Group in the Swiss Alps and for the northern Tien Shan in Kazakhstan and Kyrgyzstan" (p. 38).

Another interesting investigation regarding glacier variation was conducted using data from Indian Remote Sensing satellites by Kulkarni et al. in 2007. "This investigation was carried out for 466 glaciers in the highly glaciered Himalayan basins, namely Baspa, Parbati and Chenab" and "has shown overall 21% reduction in glacial area from the middle of the last century. Mean area of glacial extent was reduced from 1.4 to 0.32 sq. km between 1962 and 2001". Nevertheless, "the number of glaciers has increased between 1962 and 2001" (due to fragmentation), but the "total areal extent has reduced" (pp. 73-74).

In the same year, glacier changes in the Alps were observed by satellite in research conducted by Paul et al. and the "qualitative analysis of multispectral satellite imagery revealed clear but indirect evidence of massive glacier down-wasting in the European Alps since 1985. The changes can easily be detected with animated

multitemporal false colour images which only require relative image matching" (2007, p. 120).

Furthermore in 2007, the old topographic maps of Svalbard and a modern digital elevation model were compared by Nuth et al. to study the glacier geometry and elevation changes on Svalbard (seven regions for a total of about 5,000 km^2) over a long time interval (54 years), showing a significant area decrease and loss of mass for the 1936-1990 period.

Still in the same year, starting from the consideration that "Alpine glaciers dynamics may serve as an indicator of Climate Change", the results of research aimed at developing "a true temporal GIS able to manage, visualize and analyse" different type of data which require a synthesis were exposed by Villa et al. Particularly, the aims to create a complex and articulated geodatabase were resumed in an "analysis of mass balance in relation to geographic parameters (aspect, slope, bedrock morphology, ice thickness), moraines mapping and analysis to support field reconstructions, mapping of different kind of features (seracs and crevasses i.e.) to support glacier dynamics analysis. Furthermore, it can be a useful base point for a web-mapping use of this data (environmental paths, geosites descriptions etc.). Moreover a more integrated quantitative analysis can be carried out by the use of a geosensors network" which can be defined as a system of tools "to acquire different kind of spatio-temporal data. GPS, total stations, digital cameras, laser scanners can be therefore defined as geosensors. GIS will be able to integrate this network of several sensor data type, offering to the research an added value in terms of a common ground for the fusion of data and in a forecasting perspective" (2007, p. 103).

Then in 2008, Malinverni et al. "developed a study process to analyse the status of some Alpine glacier groups (Adamello, Ortles-Cevedale and Bernina) localised in the North of Italy, the 'water tower' of Europe. The investigation was based on a set of three multi-temporal Landsat scenes acquired with the sensors MSS, TM and ETM+ combined with other types of information (2D, 3D and thematic data). The GIS based analysis, supported by remote sensing processing, allowed the extrapolation of the meaningful parameters for the glacier dynamism in the temporal displacement of observation" (p. 120). They showed that: "More refined classification methods, principal components analyses and image rationing can produce a classification which is supported by a rigorous accuracy assessment and can facilitate the production of accurate maps of glacier extension useful for glacier inventory, for change detection studies and also for analysing the influence of climate change and global warming. The acquired location and the extent of each glacier derived by remote sensing techniques can update the data-base, adding information about the accumulation and ablation areas from which the accumulation area ratio (AAR) can be derived. Furthermore, the integration of the digital elevation model with the dataset could facilitate the derivation of some other important glacier inventory attributes" (pp. 130-131).

One year later, Knoll and Kerschner applied a "new approach to glacier inventory, based on airborne laser-scanner data", to South Tyrol (Italy): "it yields highly accurate results with a minimum of human supervision. Earlier inventories, from 1983 and 1997, are used to compare changes in area, volume and equilibrium-line altitude. A reduction of 32% was observed in glacier area from 1983 to 2006. Volume change, derived from the 1997 and 2006 digital elevation models, was –1.037 km^3" (p. 46). So, modern Earth-observation methods and technologies (laser-scanning and radar remote sensing) have shown their importance for estimating and monitoring variations recorded in areas and volume, offering interesting "opportunity to investigate glacier changes" (2009, p. 50).

In 2010, Bolch et al. provided "a comprehensive multi-temporal glacier inventory for British Columbia and Alberta, a region that contains over 15,000 glaciers, for the years 1985, 2000 (for about half of the area) and 2005, generated in a time frame of less than 1 year". Regarding the technologies and tools used, they worked with satellite imagery, DEM and digital outlines of glaciers from 1985 and the results showed that: "Glacier area in western Canada declined 11.1±3.8% between 1985 and 2005. The highest shrinkage rate in British Columbia

was found in the northern Interior Ranges (−24.0±4.9%), the lowest in the northern Coast Mountains (−7.7±4.6%). The continental glaciers in the central and southern Rocky Mountains of Alberta, shrank the most (−25.4±4.1%). However, the shrinkage rate is mostly influenced by glacier size. Regional differences in ice loss are smaller when glaciers of any given size class are examined […]. The shrinkage rates have possibly increased across the study area in the period 2000–2005, with the highest increase in the Rocky Mountains" (pp. 135-136).

Recently, in the study conducted by Negi et al. "Gangotri glacier [Himalaya, India] was monitored using Indian Remote Sensing (IRS) LISS-III sensor data in combination with field collected snow-meteorological data" for the period 2001-2008 (2012, p. 855), testing the potentialities and add value of the satellite remote sensing for a temporal interval of seven years. "The observed changes in snow cover area and snow characteristics were validated using field collected snow-meteorological data and field visit" (p. 864). The results of the investigation underlined an "overall decreasing trend in the areal extent of seasonal snow cover area (SCA)" (p. 855) and confirmed "the retreat of Gangotri glacier" (p. 864). Moreover: "This study has shown that the changes on glacier surface are due to climatic and topographic (local geomorphology) factors, which decreased overall glaciated area by 6% between 1962 and 2006" (p. 864).

Another contemporary paper, using also false colour images which have demonstrated their importance both in snow mapping and in identifying various glacial landforms, presented "the results obtained from the analysis of a set of multitemporal Landsat MSS, TM and ETM+ images for the monitoring and analysis of Gangotri Glacier main trunk change". The investigation and data analysed by Haq et al. have shown an overall significant reduction in glacier area between 1972 and 2010 (2012, p. 259).

Owing to its relevance and numerous applications, it is worth noting the "GLIMS" project *(Global Land Ice Measurements from Space)* coordinated by Jeffrey S. Kargel and finalised "to monitor the world's glaciers primarily using data from optical satellite instruments, such as ASTER (Advanced Spaceborne Thermal Emission and reflection Radiometer)" (http://www.glims.org).

In fact, the main applications of GLIMS concern (http://www.glims.org/About):

- *Global Change Detection* and "GLIMS' mission to establish a global inventory of ice will provide the community with data for later comparison. Monitoring glaciers across the globe and understanding not only the cause of those changes, but the effects", the project will provide important steps "to a greater understanding of global change and its causes";
- *Hazards Detection and Assessment* because "outburst floods, landslides, debris flows, and debris avalanches can destroy property and take lives in a sudden rush of water, ice, sediment, rock, soil, and debris", provoking relevant problems and damages to the communities exposed to risk;
- *Glacier Monitoring* and "through the long-term monitoring of the world's glaciers" the GLIMS project has also the purpose to "build a base of historical data, detect climate changes early, and predict and avoid hazards to human communities living in the proximity of glaciers".

The GLIMS project "has implemented a database of glacier outlines from around the world and other information about glaciers that includes the metadata on how those outlines were derived" (http://www.glims.org/glims blurb.html). The GLIMS database is thought "to be a logical extension of the World Glacier Inventory (WGI) of the World Glacier Monitoring Service (WGMS)" (http://nsidc.org/glims/). For more than a century, WGMS and other predecessor organizations "have been compiling and disseminating standardized data on glacier fluctuations". Particularly, "WGMS annually collects glacier data through its scientific collaboration network that is active in more than 30 countries" (http://www.wgms.ch/).

Moreover, as supplementary element, the Randolph glacier inventory (RGI 3.2) was produced, which is a global inventory of glacier outlines (http://www.glims.org/RGI/randolph.html).

However, we have to remember that interesting input and considerations for the study of glacier variation based on remote sensing were already being carried out at the end of the 70s and 80s (Rabagliati and Serandrei Barbero, 1979; Della Ventura et al., 1982, 1983; Dozier, 1984), when for example remote sensing and geotechniques for the automatic analysis of digital images were applied to evaluate the glacier surfaces of Mount Disgrazia (Alpi Retiche, Italy) and to estimate fluctuations over time (between 1975 and 1980) (Della Ventura et al., 1985). Therefore, papers like these represent "guide studies" which have provided elements and input useful for future research and developments in the general framework of knowledge.

New interesting contributions were successively produced in the 90s when:

- Landsat Thematic Mapper (TM) data of some glaciers in the eastern Alps of Austria were acquired every two years (in 1984, 1986, 1988 and 1990) and studied in detail in order to observe and quantify the glacier variations (Bayr et al., 1994, p. 1733);
- a specific algorithm was developed to map global snow cover using Earth Observing System (EOS) Moderate Resolution Imaging Spectroradiometer (MODIS) data (Hall et al., 1995, p. 127);
- the capability and potentialities of Spaceborne Imaging Radar-C/X-band Synthetic Aperture Radar (SIR-C/X-SAR) to map seasonal snow covers in alpine regions were tested (Shi and Dozier, 1997, p. 294);
- the SIR-C/X-SAR was used to map snow and glacial ice on the rugged north slope of Mount Everest (Albright et al., 1998, p. 25823).

Also at the beginning of 2000 a great amount of increasingly detailed research on these topics was published and relevant contributions were for example focussed on the Swiss and Austrian Alps.

Particularly, in 2000 a methodology based on remote sensing for analysing the distribution of glacier mass-balance was presented by Hubbard et al. as far as concerns Haut glacier d'Arolla (Valais, Switzerland, between September 1992 and September 1993).

In 2001 aerophotogrammetric techniques and data and DEMs were used by Kääb to reconstruct a 20-year mass-balance curve (1973-1992) of Grubengletscher (Swiss Alps).

In 2002 a trend analysis of glacier area between 1969 and 1992 was conducted by Paul for 235 glaciers in the Tyrol (Austria), using Landsat Thematic Mapper (TM) imagery and data from the Austrian glacier inventory and the results showed that: "The total loss in area in this period is about 43 km^2 or -18.6% of the area in 1969 (230.5 km^2). Glaciers smaller than 1 km^2 contribute 59% (25 km^2) to the total loss although they covered only one-third of the area in 1969" (p. 787).

In the same year, a new Swiss glacier inventory was compiled from satellite data for the year 2000 and the most important tasks described by Paul et al. were: "(1) an accuracy assessment of different methods for glacier classification with Landsat Thematic Mapper (TM) data and a digital elevation model (DEM); (2) the geographical information system (GIS)-based methods for automatic extraction of individual glaciers from classified satellite data and the computation of three-dimensional glacier parameters (such as minimum, maximum and median elevation or slope and orientation) by fusion with a DEM" (2002, p. 355). This work, applying different glacier-mapping methods, has shown the relevant role obtained by the synergic interaction between remote sensing and GIS in a context where the digital elevation model can provide other useful information and offer almost two main functions: "the orthorectification of the satellite imagery, and the derivation of three-dimensional glacier parameters within a GIS" (p. 358).

And then again in 2002, another study connected with the previous one and conducted by Kääb et al. concluded that: "The new Swiss Glacier Inventory 2000 confirms the clear trend in area-loss of Alpine glaciers. A drastic acceleration of retreat since 1985 can be

observed for the entire glacier sample analysed here (< 10 km^2). Although this drastic area loss of small glaciers is not equivalent to drastic volume loss with respect to the total ice volume […] it has significant effects on processes involved in surface energy balance, hydrology or landscape evolution. The behaviour of the small glaciers shows a high spatial and temporal variability which can completely be assessed only by remote sensing methods".

Regarding aerophotogrammetric techniques applied to glacier inventory and studies on relationships between glacier changes and climate evolution, two recent studies combining registered colour orthophotos with differential GPS (DGPS) field measurements described the evolution of the two most glacialized Italian regions (Aosta Valley and Lombardy). Diolaiuti et al. recorded a mean area loss of Aosta Valley glaciers during 1975-2005 of about -27% (-9% per decade) (2012a, p. 17). In Lombardy glaciers' area reduced from 1991 to 2003 by 21% and glaciers "smaller than 1 km^2 accounted for 53% of the total loss in area" (Diolaiuti et al., 2012b, p. 429).

To add some other recent results based on remote sensing methods, it must be remembered that Mihalcea et al. tested in 2008 the possibility of using ASTER satellite and ground-based surface temperature measurements to derive supraglacial debris cover and thickness patterns on debris-covered glaciers. "The comparison between field and remotely sensed data serves four purposes: 1) to compare different temperature data sources, assessing their reliability and accuracy; 2) to assist in the interpretation of the spatial variations of surface temperature on a debris-covered glacier; 3) to develop a method for mapping supraglacial debris cover distribution and thickness from ASTER data; 4) to assess the validity of the satellite-derived debris thickness map using field debris thickness measurements" (p. 342). The results obtained on Miage glacier confirmed the "validity of ASTER-derived surface temperatures of debris-covered" (p. 353).

Moreover, a contribution to analyse some particular glacier evolutions (i.e. the "Karakoram anomaly", where a situation of general stability has been recently depicted) has been added by Minora et al. in 2013. They focussed "the attention upon the glacier evolution within the Central Karakoram National Park […] to assess the magnitude and rate of such anomaly". Using remote sensing data (for example Landsat images), they "analyzed a sample of more than 700 glaciers" and "found out their area change between 2001 and 2010 is not significant (+27 km^2 ±42 km^2), thus confirming their stationarity" (p. 2892).

To sum up, literary review shows that remote sensing is a powerful tool for the study of glaciers from many points of view and it can be used in a synergic approach with GIS, GPS and other geospatial technologies.

It also represents a very useful didactical tool making it possible to:

- understand mountain and glacial environments and recognize peculiar forms and elements which in many cases would require lot of direct experience acquired during field surveys to be acknowledged;
- see with one's "own eyes" the changes recorded over time in terms of areas affected by glaciers;
- search for common points and different elements among mountain environments and glaciers;
- understand the hazards related to particular aspects of glacier environment in high mountains;
- visualize images with strong "visual impact" which can capture the attention, stimulating hypothesis, considerations, dynamic participation in class and lively discussions with classmates and teachers;
- promote laboratorial and professional didactics, a kind of start-up of research in didactics and research for didactics, which represent crucial points, an essential symbiosis to show and spread the "real face" of modern geography.

From the didactical perspective, some examples of image visualizers from the air and satellites for the study of mountain environments, which highlight the differences between various contexts, have been given by

De Vecchis and Pesaresi in 2011 (pp. 79-90), also comparing this kind of images with topographic maps and simulating a geography cycle of geography lessons which can be supported by these very interesting iconographic materials.

New perspectives can moreover be opened up by the function of ArcGIS Online which can be added to ESRI's GIS software. In fact, thanks to this modality, it is possible to visualize many images and applications already made to be shared, satisfying relevant didactical aspects concerning: the availability of the images; the overlay of related layers which use different sources or referred years, permitting the monitoring of glacier retreats and variations; the observation of prepared elaborations which can also provide input for similar elaborations and for new research in other contexts; the possibility of uploading one's own elaboration to share with other users, giving enthusiasm and increasing the sense of responsibility of single students and the group working on the research. Further important applications can be obtained by the integration between satellite images and GIS, importing georeferenced images in a GIS software able to re-elaborate, analyse and compare the acquired images. Thus, by the combined use of various geotechnologies it is possible to undertake many interesting didactical investigations, promoting and supporting innovative interdisciplinary studies, where specific methodologies and tools can be tested.

3. Miage glacier

The Miage glacier is a typical debris-covered valley glacier of the upper Veny Valley (Aosta Valley, Italy), that drains the southwest slope of the Mont Blanc massif. A *valley glacier* means that the ice body has such a long tongue as to flow along a valley. A *debris-covered glacier* means a glacier where part of the ablation zone has a continuous cover of supraglacial debris across its full width. Some authors apply a more rigorous definition of debris cover over at least 50% of the ablation zone (Kirkbride, 2011). This can greatly influence ablation values all over the glacier. In particular, a thin and dispersed layer of supraglacial debris is able to enhance ice melting above clean or uncovered ice rates because low-albedo rock surfaces absorb much of the incoming short-wave radiation (Kirkbride, 2011). On the contrary, under a continuous clast-thick cover, exceeding a "critical value" (Mattson et al., 1993), heat transfer to the debris-ice interface is reduced due to the low thermal conductivity of the void-rich debris layer (Kirkbride, 2011; Nakawo and Rana, 1999; Adhikary et al., 2000; Mihalcea et al., 2006; Mihalcea et al., 2008; Scherler et al., 2011). With its 11 km^2 of surface, Miage represents the largest glacier of the Italian side of the Mont Blanc, and the third in Italy (after the Adamello and Forni glaciers).

The Miage glacier can be divided into three distinct zones: i) the upper part, characterized by numerous steep and narrow ice confluences, ii) the central part, almost flat, where the glacier tongue is canalized between steep slopes, and iii) the lower part, which flows into the Veny Valley, flanked by the Little Ice Age lateral moraine system.

The main flow line goes linearly North-West to South-West, bending in the very last portion to become parallel to the valley profile (SW-NE). The glacier extends from around 4,800 m a.s.l. (top of Mont Blanc) down to 1,770 m a.s.l.

The supraglacial debris cover of the Miage glacier mainly derives from landslides, and it is then redistributed by ice flow and snow avalanches all over the ablation tongue. Debris thickness increases from a few centimeters of dispersed cover on the upper tongue to >1 m at the terminus at 1,770 m a.s.l., although debris cover is patchy or absent in localized areas of crevasses (Brock et al., 2010; Diolaiuti et al., 2005; Deline, 2005). The different distribution and thickness of the supraglacial debris cause an increase of the so-called "*differential ablation*" (i.e. the ratio between the melt rate of debris-free ice and that occurring at debris-covered ice at the same elevation). Debris distribution (together with its different size and lithology) can lead to peculiar geomorphological features of the glacier surface. Among others, medial moraines, glacier tables, dirt cones, and cryoconites are the most common epiglacial features found on the Miage glacier (Smiraglia and Diolaiuti, 2011).

A marginal ice-contact lake is also present, near the southern extremity of the Miage glacier.

The ice-water contact increases calving rates of the glacier cliffs, possibly leading to flood hazards and consequently calving waves. Thus, lake monitoring is very important for visitors' safety, as it represents a popular tourist destination. For this purpose, we recall the tragedy that was avoided of 1996, when 11 tourists close to the lake got seriously injured because of a calving wave generated by an enormous ice wall which suddenly separated from the glacier and fell into the water below.

3.1 Analysis of the Miage glacier satellite images

The sector of the Western Alps where the Miage glacier is located is illustrated in this satellite medium resolution image (Figure 1), acquired on 18 April 2013 by the Operational Land Imager (OLI) instrument, carried by the Landsat-8 satellite, and visualized in natural colours. The dendritic appearance of the French, Swiss and Italian valleys in the North-Western Alps is well depicted in greenish-brownish colours. The Landsat scene covers an area of 180x180 km^2, from lake Geneva (top-left) to almost Turin (bottom-right), where the Aosta Valley rising from Turin towards the centre of the image and the opposite valley of the river Arve rising from Geneva arrive from opposite directions to the Mont Blanc massif in the center-left of the image. The Miage glacier can be recognised in this winter image as a very narrow white oblique line NW-SE between the end of the two valleys (zooming electronically the image would facilitate the analysis).

The same Landsat-8 multispectral image but in a different band composition is shown in Figure 2. Here, the false colours come from the RGB 753 visualization, that is to say by displaying the Band 7 (Short Wavelength Mid Infrared [MIR] at 2.100-2.300 µm in Red colour, the Band 5 (Near Infrared [NIR] at 0.845-0.885 µm) in Green colour and the Band 3 (Green Visible at 0.525 – 0.600 µm) in Blue colour. This false colour combination has the advantage of showing ice in tones of light blue (that means no Red nor Green colours, therefore very little reflected radiation by MIR and NIR spectral bands), thereby giving an immediate idea at first glance about ice and snow (white) coverage in the area and their topography. In this image, the Miage glacier can be recognised as a bright light blue segment in the NW-SE direction between the two valleys mentioned above.

Focusing on the glacier itself, an ALOS multispectral satellite image, acquired during the summer season on 31 August 2009 and visualised with band combination 431, is analysed (Figure 3). The scene includes all the glaciers belonging to the Mont Blanc massif, both on the Italian side and the French one. Figure 3 is a FCC (False Composite Colour) image, namely a combination of two visible (3, 1), and one NIR (Near InfraRed) (4) satellite bands in the RGB colour model (i.e. R=4; G=3; B=1). The resulting colours are:

i) red for vegetation (as visible wavelengths are highly absorbed by plants and NIR (band 4) radiometric values are visualized in the Red channel);

ii) greysh-blueish for rocks (and debris) (the latter making the distinction between debris covering ice and debris without ice below not so easy) , and very dark blue for water (see supraglacial small lakes and the ice contact lake) (because the latter has high absorption for the radiation in these three spectral bands);

iii) light blue for ice (well detectable on the ice falls or seracs);

iv) white for snow (i.e. total reflection, both for visible and NIR wavelengths) (only small avalanches patches on both the flanks of the valley and the upper zones of the ice confluences).

The Miage glacier is immediately recognizable owing to its peculiar shape (see in particular the three lobes of the terminus) and for being the unique glacier to be almost totally covered by debris. It is in fact one of the largest debris-covered glacier in the Alps (Deline, 2005). Moreover, in Figure 4 the absence of a real and large accumulation basin in its upper section can be clearly seen, while its accumulation is mainly based on the avalanches deriving from numerous narrow ice tongues (Mont Blanc, Dome, Bionassay, Col du Miage, Tète Carrée) flowing into the main ice body. Those characteristics make it easy to define the Miage glacier as a

Himalayan-type glacier. Clearly visible are the medial moraines, which below form tributary confluences between 2,500 and 2,600 m a.s.l., and then develop into continuous debris cover below 2,400 m a.s.l., which has a varied lithology dominated by schists and granites on the western (dark grey on the image) and eastern sides (light grey) of the tongue, respectively. It is easy to observe that the glacier surface has not significantly retreated with respect to the Little Ice Age maximum, as attested by the lateral moraines, much less than at nearby debris-free glaciers owing to the insulating effect of the debris cover.

At the southern limit of the glacier, just where the ice stream turns sharply toward North-East, the ice contact lake (Miage lake) is also well visible. In the image the lake appears to be composed of two distinct parts.

The one in contact with the glacier is light blue, is almost empty and supplied by glacier melting water.

The colour depends on its turbidity, which absorbs only a little quantity of sunlight, thus strongly reflecting it back to the satellite sensor. The southern part of the lake appears dark blue instead, due to the absence of the direct ice melting water supply. That is to say, a turbid water is more reflective than clear water at all visible and near infrared wavelengths (Moore, 1980). Moreover, the different colours of the two parts of the lake indicate there is likely to be no connection between the two zones.

In facts, bathymetric surveys showed that the lake consists of two basins separated by a largely submerged moraine (Diolaiuti et al., 2005). The lake is characterised by rapid drawdown episodes that have occurred with varying frequency in its history. The last rapid draining event (September 2004) was probably caused by sudden and temporary failure in the ice floor (Masetti et al., 2009).

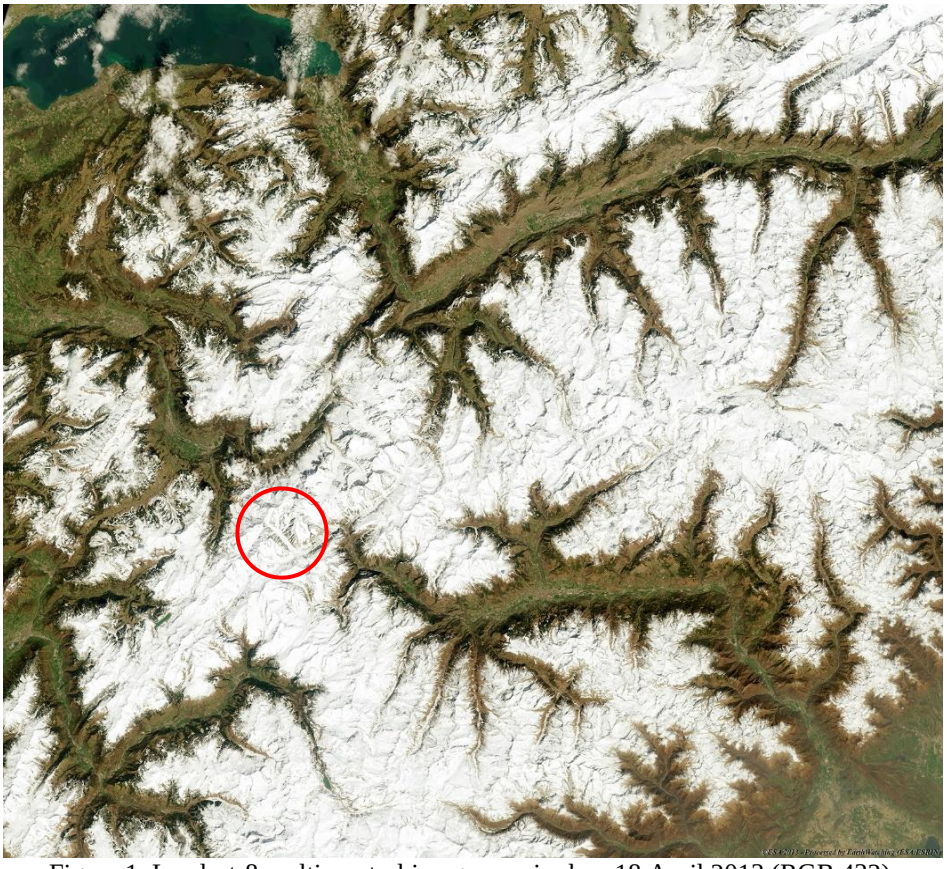

Figure 1. Landsat-8 multispectral image acquired on 18 April 2013 (RGB 432). Source: ESA.

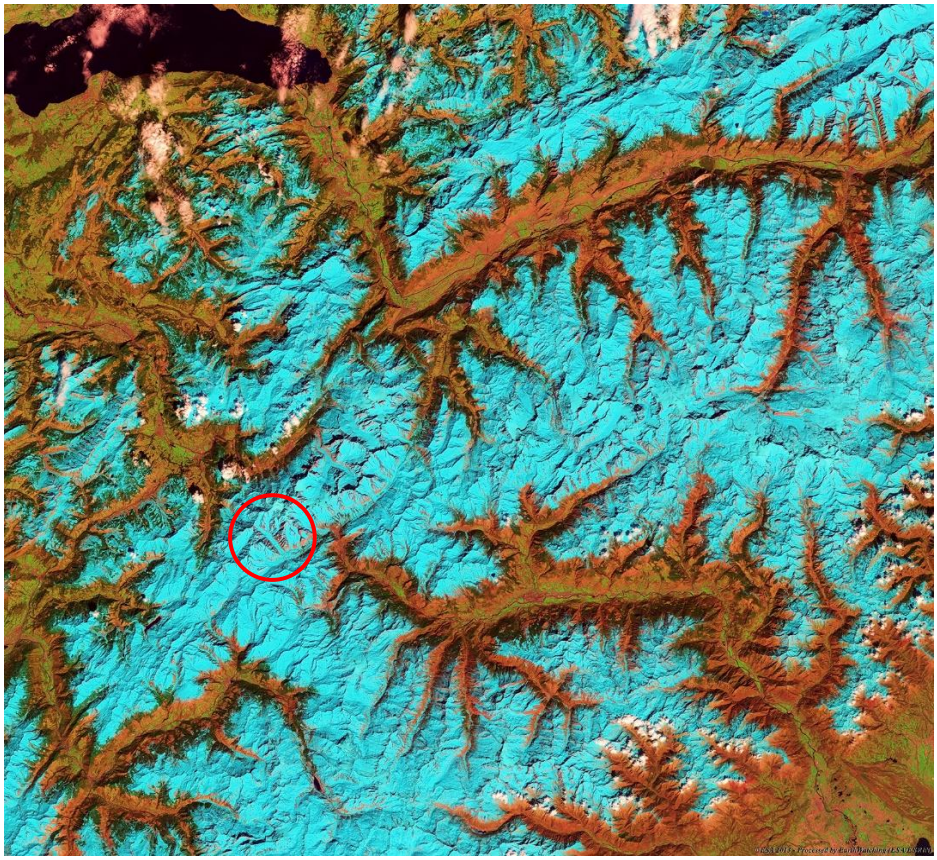

Figure 2. Landsat-8 multispectral image acquired on 18 April 2013 (RGB 753).
Source: ESA.

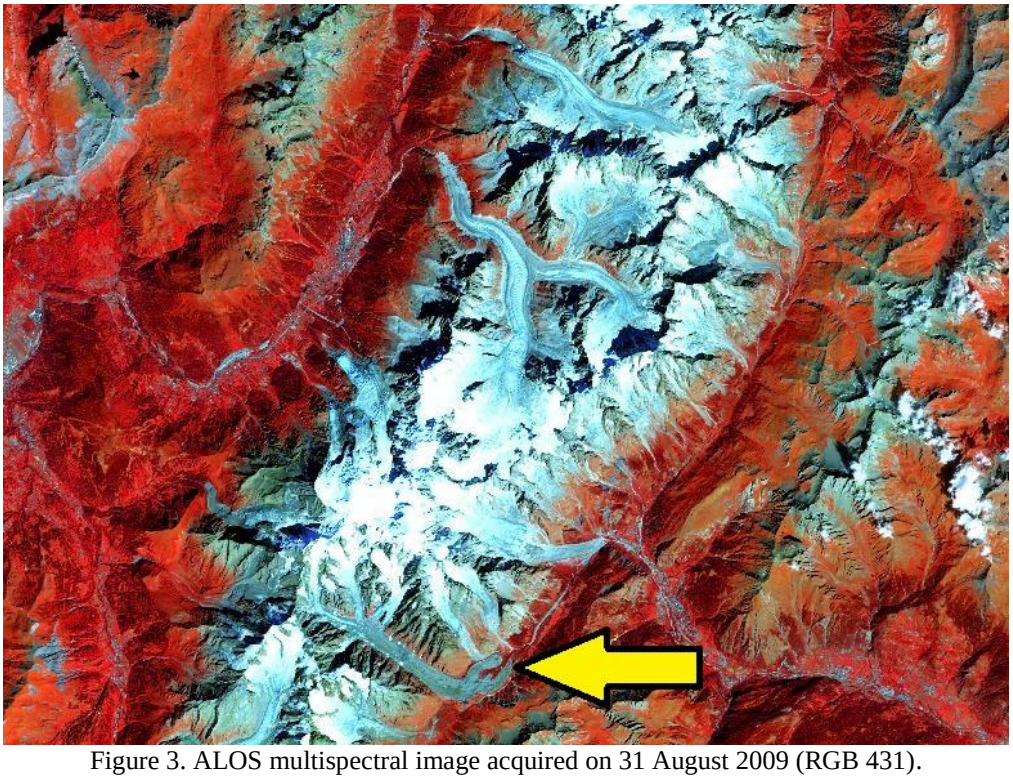

Figure 3. ALOS multispectral image acquired on 31 August 2009 (RGB 431).
Source: ESA, JAXA (Japan Aerospace Exploration Agency).

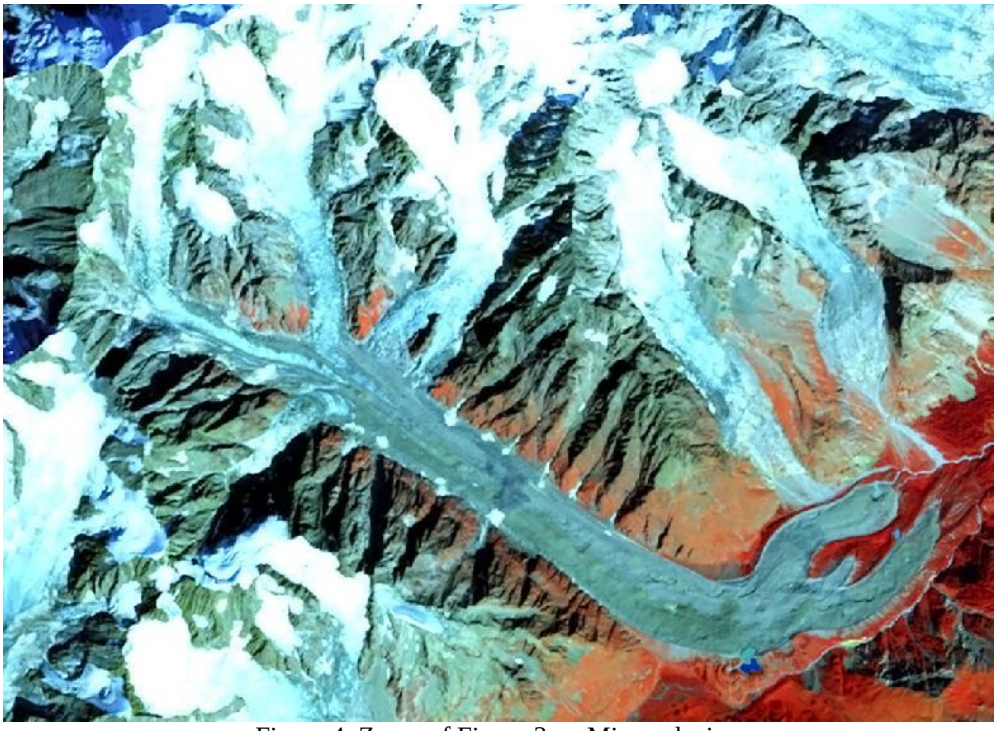

Figure 4. Zoom of Figure 3 on Miage glacier.
Source: ESA, JAXA.

4. Freney glacier

The Freney glacier is a steep mountain glacier of the Mont Blanc massif (Graian Alps), in the upper Veny Valley, close to Courmayeur (Aosta Valley, Italy). A *mountain* glacier, contrary to a *valley* glacier is a glacier type that has no tongue or only a short one and does not flow down enough to reach the main valley. The Freney flows down the southern side of Mont Blanc de Courmayeur, between the ridge of Peuterey and the ridge of Innominata, along a deep narrow hanging valley. The ridge of Innominata separates it from the twin glacier of Brouillard, that flows parallel to it. Not far from the Freney glacier, the two main debris-covered glaciers of the Italian Mont Blanc massif (Miage southwestward) and Brenva (northeastward) extend their long black tongues. The discharge waters of these glaciers together feed the Dora di Veny River, which flows into the Dora Baltea River and finally into the well-known Po river.

The Freney glacier covers a surface of about 1.4 km^2 and its length is of 2.3 km *ca*. It extends from 3,700 m to around 2,400 m a.s.l. Above, within a small cirque, there is a *glacieret* (a very small glacier or ice masse of indefinite shape in hollows which has little or not movement for at least two consecutive years) which discharges ice into the Freney glacier below feeding it and until the 1970s was still connected with the main trunk. Even during the peak of the Little Ice Age the Freney glacier did not reach the main bottom valley of Val Veny and its snout remained hanging on a steep rock belt. At present the snout is very thin and flows down up to a few score meters from the rock step where a small frontal moraine has been deposited. The entire surface of the glacier is broken and dissected by a grid of crevasses and seracs. The Freney could represent a significant sample of small size glacier (around 1 km^2); concerning this type of glaciers, one debated argument is about their fate in the forthcoming decades in the context of climate change. Italian glaciers underwent a generalized retreat in the 20th century (Citterio et al., 2007) and in particular the Aosta Valley glaciers lost 44.3 km^2 during 1975-2005, i.e. c. 27% of the initial area (Diolaiuti et al., 2012a). Small glaciers contributed considerably to total area loss; in fact the smaller the glacier the faster the reduction in size, so their extintion is more

than a mere conjecture. On the other hand, glaciers flowing down along a narrow valley in steep mountain topography, such as the Freney, are subject to a slightly stronger shading. So, these shrinking glaciers are becoming less sensitive to climatic change and might thus be able to stabilize their extent. In any case, the southward aspect and the climatic forcing on one hand, and the protecting shading effect of vertical peaks on the other hand, could play opposite roles in the Freney glacier fate, and therefore it is hard to make any prediction.

4.1 Analysis of the Freney glacier satellite images

The Freney glacier is located very close to the Miage glacier, so that in the Landsat-8 images used to illustrate this alpine region (Figures 1 and 2), it can be identified almost parallel to it, just on the right hand side of the latter, after the Brouillard glacier, nearly touching the north-western end of the Aosta Valley, not too far from Courmayeur.

The image used here to describe the Freney glacier is the same one utilized for the Miage glacier, namely an ALOS (Advanced Land Observing Satellite) scene acquired on 31 August 2009 (Figure 5, left part). In Figure 5, glaciers are represented in light blue colour and snow in white, while rocks (and debris) are grey and vegetation is red. This colour contrast is due to the RGB combination of bands 431 of the AVNIR-2 (Advanced Visible and Near Infrared Radiometer type 2) sensor, and this allows an easy identification of glacier bodies.

It is not difficult to identify the snow line that divides the accumulation basin (the white narrow upper cirque) from the ablation basin (the light blue tongue): note the grey debris cover on the lowest part of the ablation basin, which has increased in the last decade, due to more effective cryogenic processes on the granite bare rock walls of Mont Blanc. The debris cover is quite complete and diffused on the lower zone of the ablation basin, while in the medium zone of the glacier it is reduced to two lateral active moraines, supplied by the debris production of the lateral rock walls.

In spite of the quite similar colour of debris still covering ice, of deposited debris and rocks, it is not particularly difficult to detect the exact glacier terminus position; the different grey tone of supraglacial debris (darker because of the higher humidity) and the evident ice step of the snout makes the glacier lower limit easily identifiable. The convex features of the terminus are also evident due to differential ablation (i.e. the ratio between the melt rate of bare or debris free ice and the melt rate occurring at debris-covered ice at the same elevation). The ablation gradient is opposite to that due to altitude, and the ice melt rate is smaller at lower altitude than that of the bare ice at higher altitude; therefore supraglacial convex morphologies began to develop and are well detectable on satellite images.

Although Landsat satellites are more utilized for glacier studies, ALOS has a higher spatial resolution (10 m against 30 m of the NASA satellites), and therefore is more suitable to study such a small glacier as the Freney one. Otherwise spatial resolution would not make it possible to recognize glacier outlines properly.

As said above, the fate of the Freney glacier is uncertain, therefore the study of remotely sensed high resolution images taken at periodic intervals is necessary to monitor its state (also taking into account the difficulty or even the impossibility of collecting reliable field data).

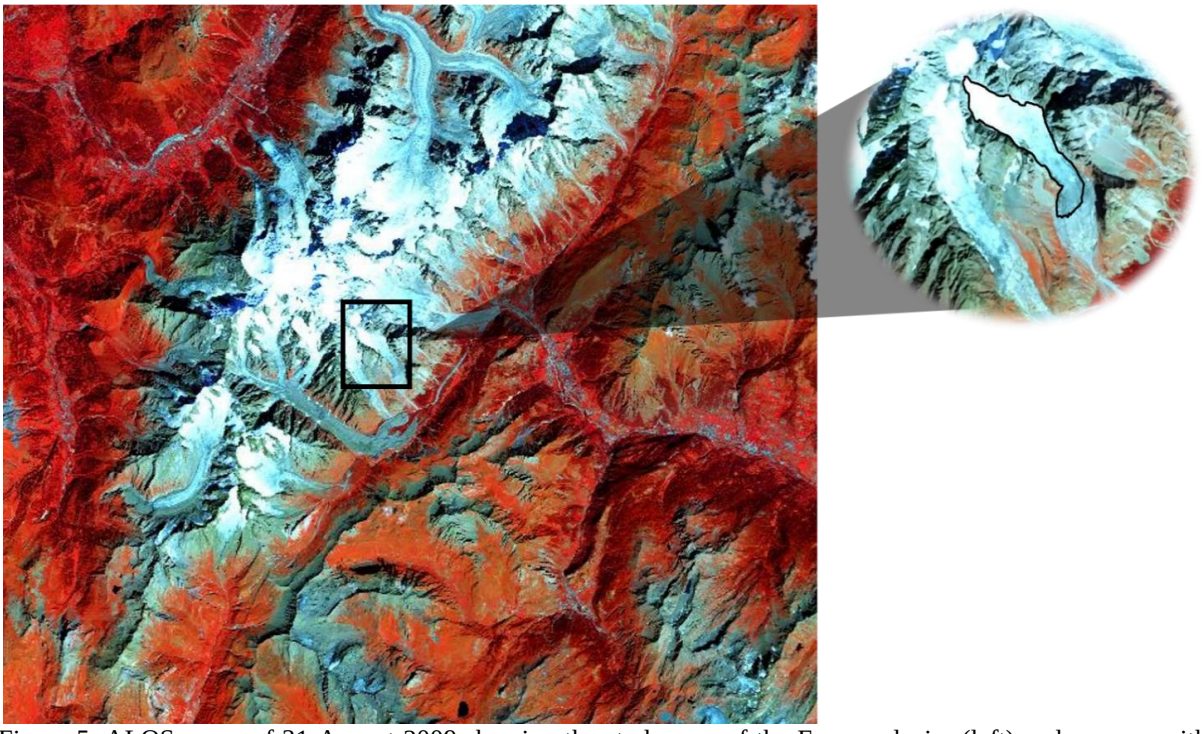

Figure 5. ALOS scene of 31 August 2009 showing the study area of the Freney glacier (left) and a zoom with black glacier outlines. Band combination is 431.
Source: ESA, JAXA.

5. Kilimanjaro glaciers

Kilimanjaro is the Africa's highest peak (5,895 m) (the "white roof of Africa"). It is a huge dormant stratovolcano located close to the Kenya-Tanzania border, 370 km *ca* south of the Equator and about the same distance from the Indian Ocean (Kaser et al., 2004). It consists of three volcanic centers, active in sequence from the Pleistocene: Shira, Mawenzi and Kibo, the latter being the highest. The summit of Kibo forms quite a flat caldera, where along the southern scarp the Uhuru Peak, the highest point of the volcano, is found and which emerges from the flat plain with its snow capped iconic bulk. Snow and glaciers of Kilimanjaro were discovered in 1848 by the German explorer Johannes Rebmann, but English geographers were incredulous about its snowcap until 1889, when Hans Meyer climbed the summit and made the first observations of glaciers.

At present, glaciers only exist on Kibo, with an extent of 1.76 km^2 in 2011, roughly half of that remaining on the continent (Hardy, 2011). The majority of the glacier bodies are bunched within two main ice fields, namely the Northern Ice Field (NIF, the largest ice body), and the Southern Ice Field (SIF). Even if from a glaciological point of view this classification (*Ice Field*) is now rather incorrect, it is still diffused and traditionally accepted. Kilimanjaro's glaciers may be distinguished in plateau or horizontal (>5,700 m) glaciers and slope (<5,700 m) glaciers. The first group on the Kibo summit has flat surfaces unbroken by crevasses; their margins are vertical or near-vertical and are fluted. The slope glaciers extend down from the crater of Kibo in only a few cases (among which Kersten glacier represents the largest remaining one, Mölg et al., 2009). They are all inclined at 30-40° and are all remnants of the former Southern Ice Field; their surface is today quite dirty, due to the wind-blow dust.

The area extent of the glaciers just prior to Meyer's observations has been estimated to be about 20 km^2 (Osmaston, 1989). So they have shrunk by more than 90 percent in little more than a century and become a global-warming poster child. The break up of ice bodies had just begun very likely at the end of the 19th century

and the drastic shrinkage continued throughout the 20th century and the beginning of the 21st century. During the last Pleistocene glaciation the extent of moraines on Kibo and Mawenzi suggests that a large ice cap blanketed the mountain, covering an area of at least 150 km^2 (Osmaston, 1989).

In spite of air temperatures always below freezing, areal reduction of plateau glaciers is caused mainly by melt on vertical walls that characterize their north and south margins, induced by solar radiation (Mölg et al., 2003; Cullen et al., 2006). The beginning of the retreat of the glaciers at the end of the 19th century can be attributed to an increase in net shortwave radiation, accompanied by a decrease in cloudiness and snowfall (Hastenrath, 2006). It appears likely that by mid-century the plateau glaciers will disappear from the mountain summit (Kaser et al., 2004; Cullen et al., 2012).

5.1 Analysis of Kilimanjaro glacier satellite images

A recent Landsat-8 satellite image dated 27 August 2013 is here used to describe the Kilimanjaro glaciers. Bands 742 are combined in the RGB model to emphasize ice and snow in the scene. In this way glaciers are indeed brought out by a bright light blue colour, in contrast with the other elements of the image (lava flows of different ages, vegetation, dry zone). In fact, Kilimanjaro's glaciers are immediately recognizable in the middle-right part of Figure 6, right in and around the volcano's crater, easily visible in the complete extent of the Landsat scene, even if it is not possible to distinguish the features of both the types of glaciers and to diversify snow from ice. The acquisition time is 11 am and afternoon clouds are coming to encircle the north-western and the southwestern slopes of the massif. This atmospheric phenomenon is more pronounced during the dry seasons and it protects ice from direct solar radiation. Thus, ablation is more apparent on the eastern margins of the cliffs than on the western ones (Kaser et al., 2004).

Figure 7 is a zoom in the crater zone, where glaciers are situated. North-West of the crater there is the NIF, while SIF is South-East. The recent longitudinal fracture of the NIF is easily detectable, splitting the ice cap in two totally separate portions. Various slope glaciers are also present down to the slopes, especially southward, ice bodies derived from the fragmentation of the SIF. NIF and SIF tall ice cliffs, and slope glaciers are very sensitive to melt/no-melt cycles. In fact, during the boreal (austral) summer north-facing (south-facing) cliffs are irradiated by direct sunlight during daytime, which provides enough energy to initiate melting at the cliff faces although the air temperature is below freezing. In contrast, during the boreal (austral) winter north-facing (south-facing) cliffs are irradiated by direct sunlight only at very low angles, thus reducing ablation significantly (Kaser et al., 2004).

6. Harding Icefield

The Harding Icefield is the largest of the icefields in the Kenay Mountains (Kenay Peninsula, Alaska) and the largest icefield entirely contained within the boundaries of the United States.

An icefield is defined as a mass of glacier ice, usually smaller than an ice cap and lacking a dome-like shape (http://nsidc.org/cgi-bin/words/glossary.pl).

The Harding Icefield is about 80 km long (northeast-southwest) and 50 km across. Including the outlet glaciers, it covers an area of about 1,800 km^2. Slightly more than half of the icefield lies within the present boundary of the Kenai Fjords National Park; the remainder lies within the Kenai National Wildlife Refuge. At least 38 glaciers of different sizes and types flow from the Harding Icefield, terrestrial and tidewater (i.e. glaciers that terminate in the sea, http://www.swisseduc.ch/glaciers/glossary/index-en.html); the most important being the Bear glacier, Exit glacier, Skilak glacier, Tustumena glacier and the Chernof glacier (Aðalgeirsdóttir et al., 1998).

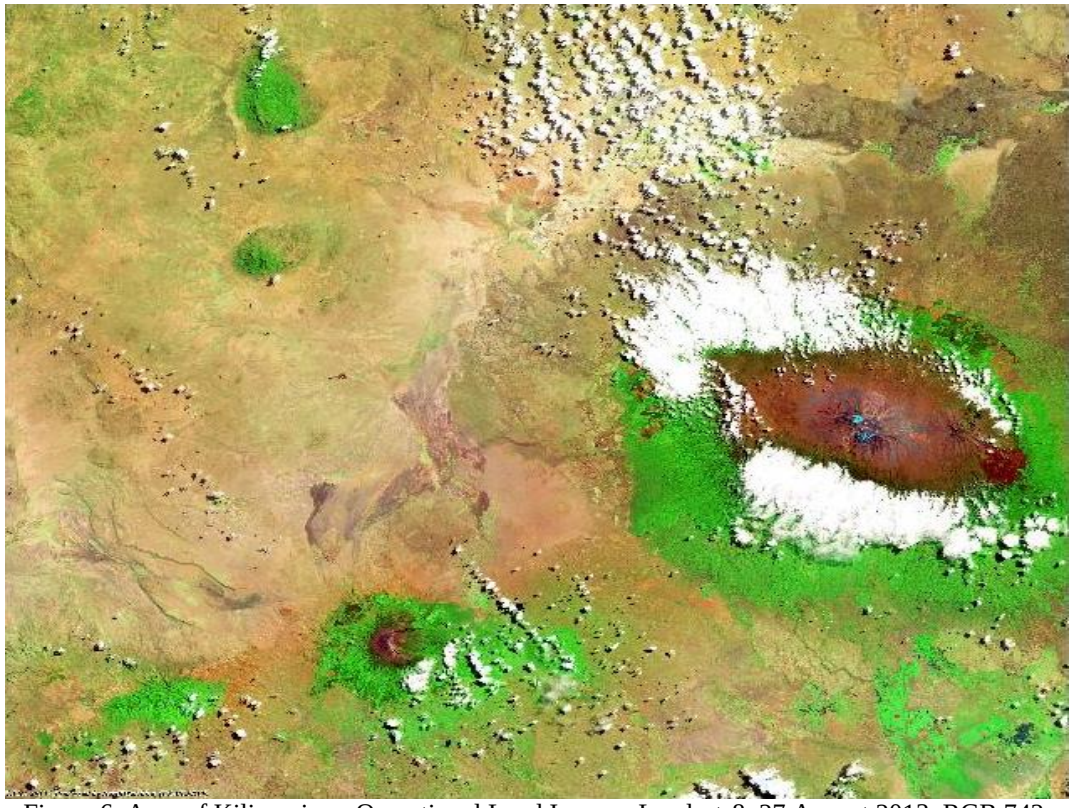

Figure 6. Area of Kilimanjaro, Operational Land Imager, Landsat-8, 27 August 2013, RGB 742.
Source: ESA.

Figure 7. Kibo's crater and glaciers therein, Kilimanjaro.
Source: ESA.

Amongst them, lake- and land-terminating glaciers are present in the west side, where the two huge lakes of Skilak and Tustunena drain some glaciers, while tidewater glaciers lie in the east. Some of the latter flow at high speed continuously (as much as 35 meters per day). Moreover, they may advance and retreat periodically, independently of climatic variation (as the *surging* glaciers, Jiskoot, 2011). Nowadays, recent studies have found that most of the glaciers in the Harding Icefield have receded (since 1973), some dramatically (Hall et al., 2005).

6.1 Analysis of Harding Icefield satellite images

The visible colour Landsat image is shown below where northeastward the smaller Sargent Icefield and southwestward the Harding Icefield are visible. Along the coast the plumes from the light grey glacial sediment are detectable as well. As the surface of the Harding Icefield is so large (1,800 km^2), Landsat resolution (30 m), is suitable for the purpose of glaciological studies in this area, even if it is impossible to describe the local morphological features such as the medial moraines. In the lower-left part of Figure 8, the Harding Icefield is well recognizable, with its tidewater glaciers on the eastern side touching the Gulf of Alaska waters. Here, the Pacific Ocean provides copious precipitation in the form of snow. On the opposite side, at the same (or higher) altitude, snow is still present but less. This is visible looking at the snow patches getting smaller as we move downward (or westward), towards the major lakes. In general, the Harding Icefield receives at least 10 meters of snow each year (http://www.kenai.fjords.national-park.com).

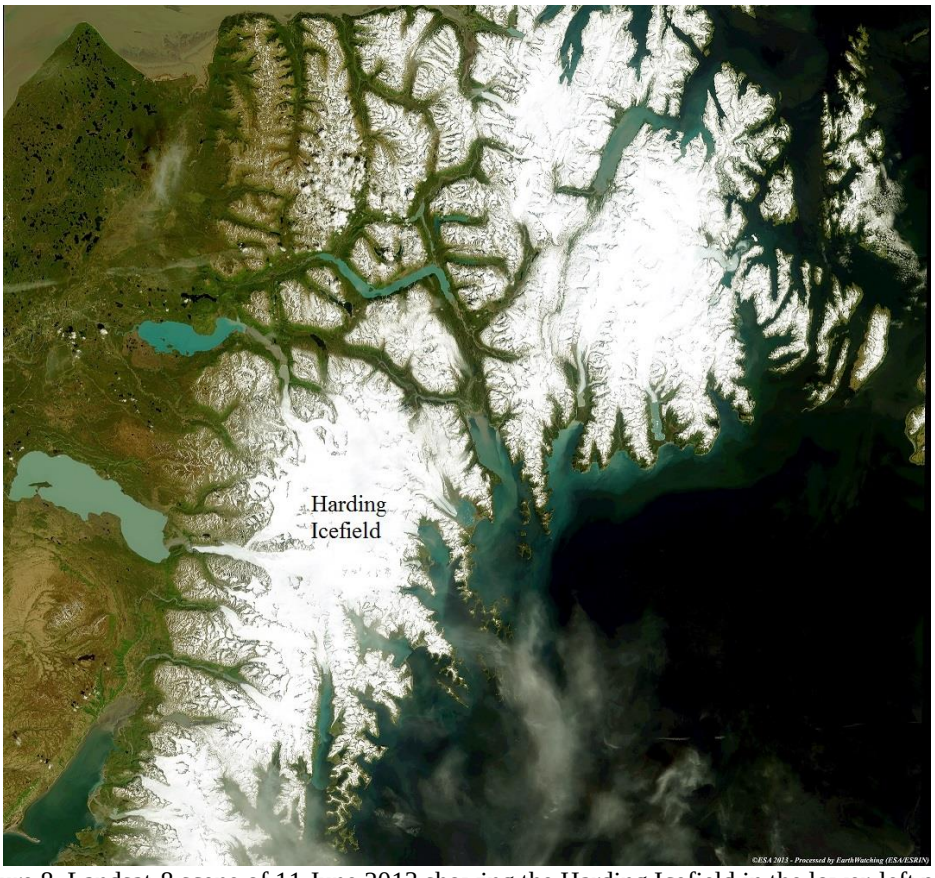

Figure 8. Landsat-8 scene of 11 June 2013 showing the Harding Icefield in the lower-left part. Source: ESA.

7. Aletsch glacier

The Aletsch glacier with a length of 23 km, surface area of about 80 km^2 and a maximum thickness of about 900 m, is by far the longest, the largest and the deepest glacier in the Alps and the most important of the Berner Alps (Valais) in Switzerland. The volume of the Aletsch was roughly 15 km^3 in 1999, representing about 20% of the entire ice volume in Switzerland (Farinotti et al., 2009). It is a typical example of compound basin valley glacier, that is to say two or more individual valley glaciers (four in the case of the Aletsch) issuing from tributary valleys and coalescing (WGMS, 2012). They all converge in the Konkordia Platz, where the ice reaches its maximum thickness of 900 m and starts the huge curved tongue (Jouvet et al., 2011). The tributary glaciers (Grosser Aletschfirn, the bigger one, the Jungfraufirn, the Ewigschneefeld and the smaller one, the Grüneggfirn) flow down into the main tongue through steep ice fall (seracs), crossed by numerous crevasses. Along the sides of the hanging valleys joining the Aletsch tongue, there is also a great amount of surface debris forming lateral moraines, a result of accumulations of debris falling from the sides due to freeze-thaw activity and glacier flow. Where the lateral moraines of these tributary glaciers join the lateral moraine of the Aletsch, medial moraines are formed, which give the glacier the appearance of being divided into neat lanes or black paths. Over the course of the twentieth century, such as most of the Alpine glaciers, the Aletsch, the largest Alpine glacier, receded by more than two km. During the Little Ice Age (between 1600 and 1860) the glacier reached its maximum area (145 km^2) and the tributary valley glaciers of Mittelaletsch and Oberaletsch still joined the main tongue. In 1957 its surface area reached 130 km^2. Then the link with the Mittelaletsch was interrupted. According to the median climatic evolution, the actual Aletsch glacier is expected to lose 90% of its ice volume by the end of 2100 (Jouvet et al., 2011).

7.1 Analysis of theAletsch glacier satellite images

The multitemporal image acquired in early Spring by Landsat-8 on 18 April 2013 (Figure 9) illustrates the southwestern part of the Central Alps, covered by snow, as a diagonal, dividing the Swiss territory on the left hand side from the Italian northwestern part of the Piedmont and Lombardy regions. The Aosta Valley penetrates the white alpine mountains from East to West just below the center of the image, whilst the Rhone Valley starts almost in the upper left corner, comes down towards the southwest and in the town of Martigny turns up to then enter lake Geneva in the area of Montreux. Mount Cervino (the Matterhorn) and Monte Rosa are located in the mid-right part of the image, and the Mount Blanc massif at one third along the south-west diagonal.

The same image, but in a false colour visualization RGB 542 (Figure 10), enhances the white alpine snow-ice coverage, the black water of the lakes and the reddish vegetated valleys.

The multispectral image acquired by ALOS on 31 July 2010 (RGB 321) (Figure 11) shows the entire Berner Alps (Swiss Alps) from the Brienzersee to the Rhone Valley, in particular the Jungfrau-Aletsch massif (a UNESCO World Heritage Site) in the center-left. Enclosed by the high summits of Aletschorn, Junfrau, Mönch and Fiescherhorn (amongst others), flows the huge Aletsch glacier with its “sword-like” shape, arriving at just some 20 km from the town of Brigue. Northeastward the other giant glaciers of the Berner Alps are well detectable with their valley tongues: Fiescher, Oberar and Unteraar (the last two with their long artificial lakes). The complex structure of accumulation basin of the Aletsch is clearly observable. Actually it is formed by four accumulation basins: clockwise the Grosser Aletschfirn represents the bigger one, then the Jungfraufirn, the Ewigschneefeld, and the smaller one, the Grüneggfirn, follow. Together they converge in the Konkordia Platz forming a semicircle, then flowing along the big curve of the ablation tongue (changing the main direction from southwestward to southeastward). They reach the glacier snout separated the one

from the other by medial moraines, well visible in the ALOS image; these moraines run along the ablation tongue like railways tracks, slightly enlarging toward the terminus, quite parallel to the lateral moraines. A visible grey line (trim-line) (Figure 12a) follows the border of the ablation tongue, indicating the limit between well-vegetated terrain that has remained ice-free for a long time and scarcely vegetated terrain that until recently (at least from the Little Ice Age) laid under glacier ice.

This image was taken in the summer period (31st of July, 2010), to limit the covering effect of the snow as much as possible. Using band combination 431 (Figure 12b) as RGB (that is to say by combining the NIR channel with two visible bands), a major colour contrast between snow (in bright white), and ice (in light blue), makes it possible to distinguish between these two features much more easily than simply looking in natural colour. Detecting the approximate position where ice makes room for snow is only possible using the FCC image (on the right of Figure 12b), while there is no way to do the same for the natural colour image (Figure 12a, on the left), because there is no change in colours. The reason why this occurs is because light is all reflected back by the albedo effect of snow and there is no radiation (colour), absorption in both images (i.e. pixel colour is white). On the other hand, ice is very weakly absorptive in the visible but has strong absorption bands in the near infrared. Thus the resulting FCC image has a greater colour contrast between snow and ice, making it possible to detect their boundary quite well. This is not only true for snow and ice, but also for the enhanced capacity to recognize glacier boundaries in the accumulation zone, or (for instance), for distinguishing mountain ridges.

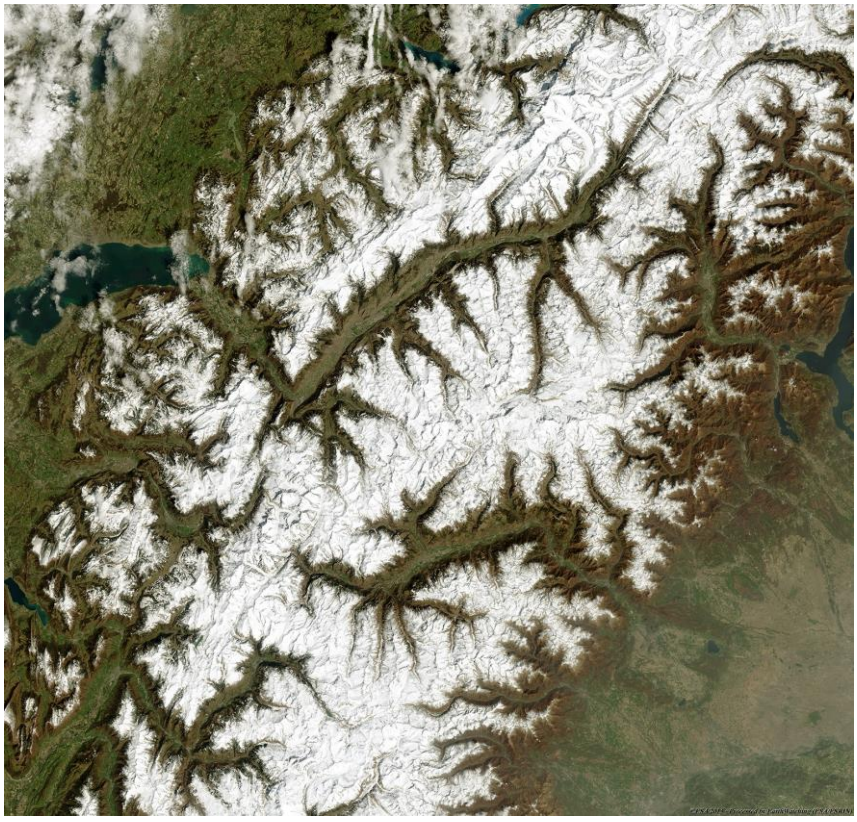

Figure 9. The western part of the Central Alps imaged by Landsat-8 on 18 April 2013 (RGB 432). Source: ESA.

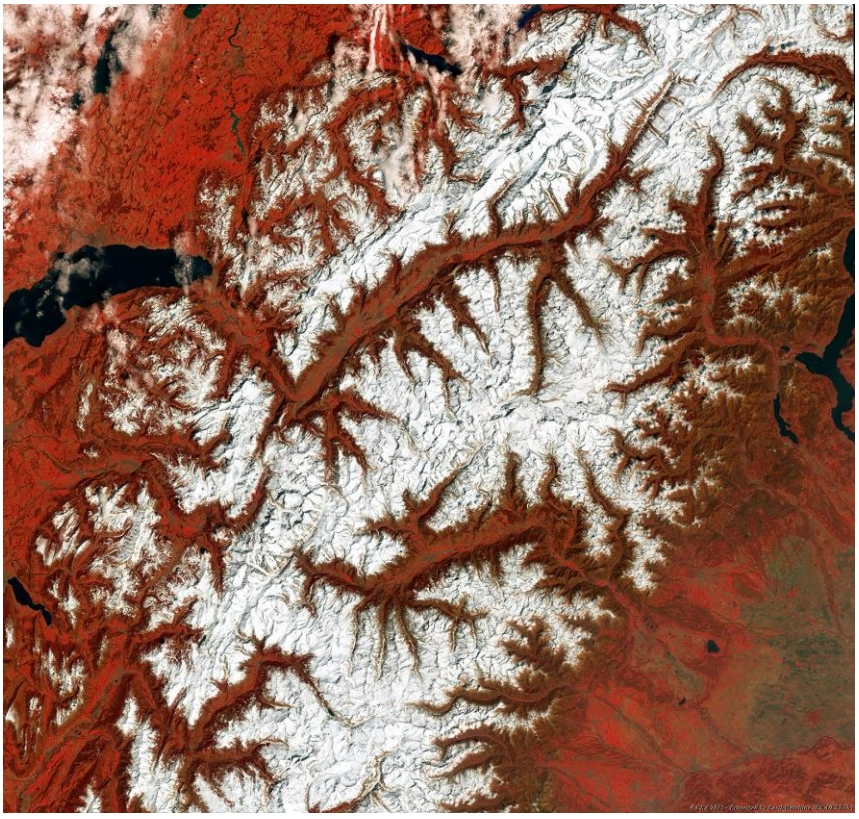

Figure 10. The same image as in Figure 9, but in a false colour visualization RGB (542).
Source: ESA.

Figure 11. ALOS image acquired on 31 July 2010 (RGB 321).
Source: ESA, JAXA.

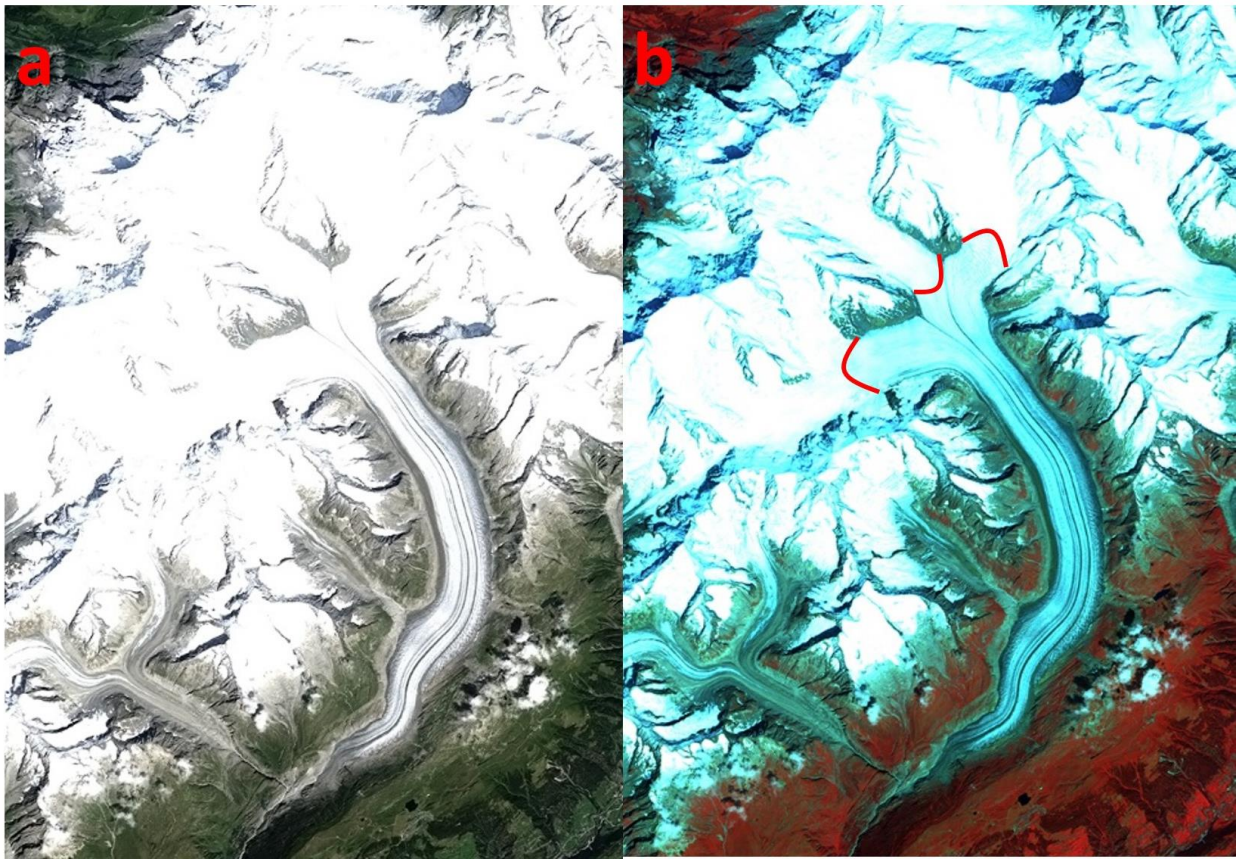

Figure 12. Aletsch glacier shown in two enlargements of the Figure 11, visualised in natural colours RGB 321 (a), and in false colours RGB 431 (b), respectively. Red lines in "b" are examples of snow-ice boundary detection.
Source: ESA, JAXA.

8. Drygalski ice tongue

The Drygalski ice tongue is the floating seaward extension of David glacier, the largest outlet glacier in the Victoria Land part of the East Antarctic ice sheet, draining from the Talos and Circe Domes of the East Antarctic ice sheet (Frezzotti and Mabin, 1994).

An outlet glacier is a tongue of ice that extends radially from an ice dome; within the dome it can be identified as a rapidly moving ribbon of ice (an "ice stream"), while beyond the dome it occupies a shallow depression (Arora, 2011).

The David glacier – Drygalski ice tongue area covers a surface of about 224,000 km^2 (Frezzotti and Mabin, 1994). The grounding line (GL: the transition between the inner grounded ice and its outer floating counterpart, i.e. where the Drygalski ice tongue begins), is about 50 km inland from the coast.

The Drygalski ice tongue floats on the west side of the Ross Sea and forms the southern coastline of Terra Nova Bay. The Drygalski tongue is fed by a faster flow (580 m per year) coming from the Circe Dome and a second slower moving flow (300 m per year) coming from the Talos Dome. These different and contrasting flow rates could probably be considered responsible for the characteristic rifts that open along the northern margin of the ice tongue (Frezzotti and Mabin, 1994).

As we move seaward starting from the David Glacier's grounding line (GL) the thickness decreases (from 1,500 to 150 m) (Tabacco et al., 2000).

The ice tongue plays a crucial role in the persistent development of the Terra Nova Bay *polynya* (area of open water surrounded by sea ice, Stringer and Groves, 1991). In fact, its formation and persistence is thought to be caused by the combined effect of the strong persistent offshore katabatic winds that prevent sea ice from forming in the bay, and the blocking effect of the Drygalski ice tongue, which stops sea ice from entering the Terra Nova Bay from the South (please, note the area of free ice water below the ice tongue in Figures 13 and 14) (Frezzotti and Mabin, 1994).

Outlet glaciers such as the David glacier, and in particular the Drygalski ice tongue, which is the part subjected to fast sea-contact dynamics, play a major role in the determination of the Antarctic ice sheet mass balance. The mass balance ablation components consist in calving and basal melting. A major *calving* event (calving is the process whereby masses of ice break off to form icebergs) occurred in December 1957, when the Drygalski ice tongue lost the outer 40 of its 110 km (estimated length from aerial photographs, Frezzotti and Mabin, 1994). Between 1997 and 2000 the Drygalski ice tongue advanced 2,200 m, increasing its area by almost 45 km^2 (Wuite et al., 2009). The basal melting rates (that is the melting at the base of the ice floating tongue) are higher close to the GL owing to thermoaline circulation by High Salinity Shelf Water. The basal melting rate is determined by the difference between net snow accumulation and ice discharge across the GL into the ocean (Frezzotti et al., 2000). About 90% of the snow that falls inland is drained by outlet glaciers and ice streams (Morgan et al., 1982). In 2005 and 2006 two huge icebergs coming from a calving of the Ross Ice Shelf collided with the ice tongue breaking off some large pieces.

8.1 Analysis of the Drygalski ice tongue satellite images

Figure 14 represents the Drygalski ice tongue as recorded by band 7 of the Landsat-8 satellite. That is to say that, it is the view of the same area as in Figure 13 (RGB 543), but filtered only through the Short Infra-Red wavelengths (from 2.11 to 2.29 μm). The result is an image where it is easier to distinguish the Drygalski ice tongue limits. Along the coast the sea ice is grey and darker with respect to the white floating ice tongues (the main Drygalski and the other minor ice tongues). The dark part of the medium Drygalski tongue and the many small other areas (that appear in light blue in Figure 13) are surfaces of the so called “blue ice”, where the wind ablation is particularly active and the snow has been blown away. In the lower sector of both the images the *polynya* is well visible and its free ice open sea contrasts with large areas of sea ice, strongly fragmented, accumulated along the northern-side of the ice tongue. This sea ice can be also multi-year ice that often remains attached to the Drygalski ice tongue for many years and is carried out into the Terra Nova Bay, giving the ice tongue the appearance of being several km wider than it really is.

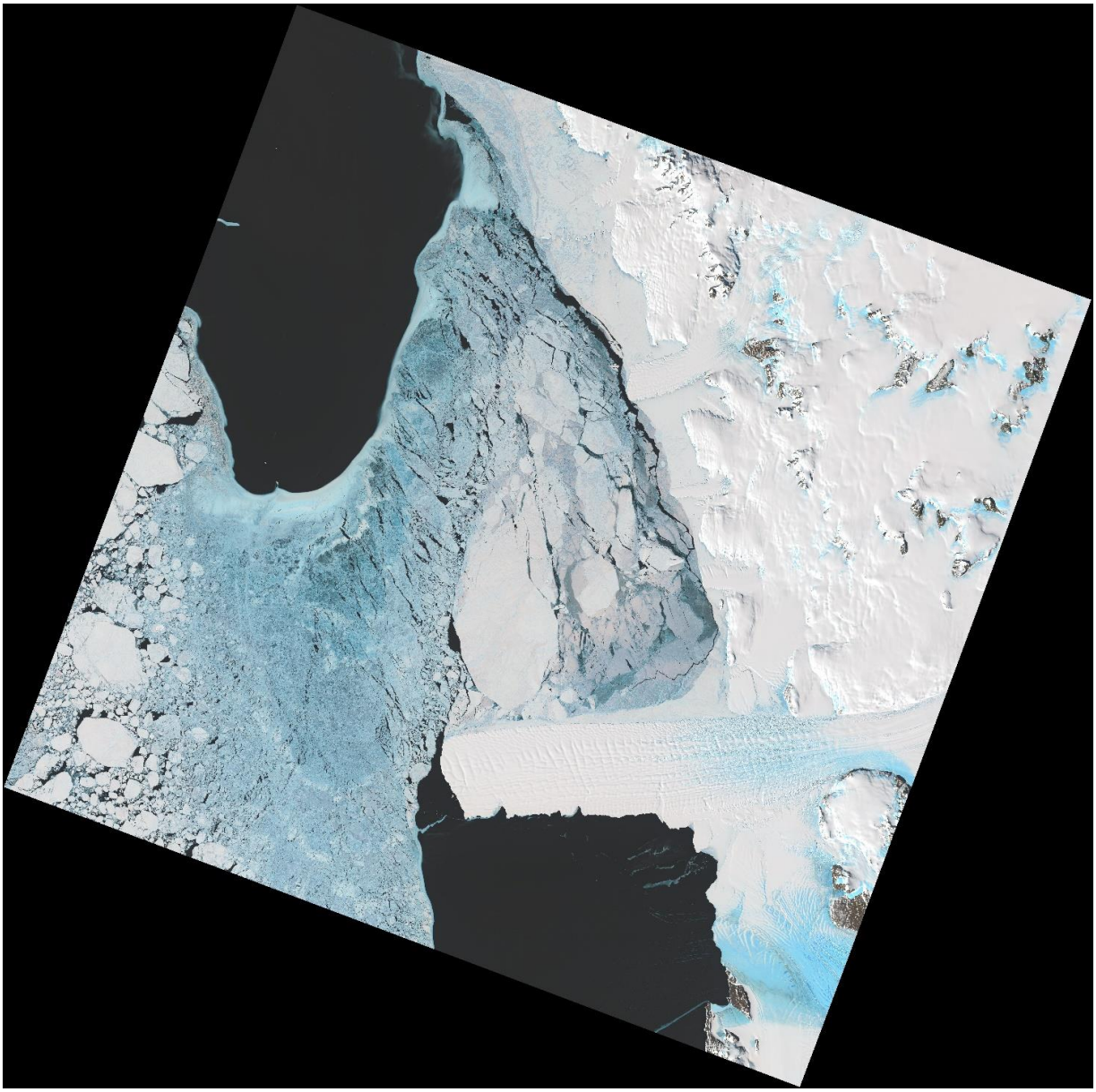

Figure 13. Landsat-8 scene of 26 November 2013 showing the Drygalski ice tongue (lower-right part). Multispectral band combination is 543.
Source: http://earthexplorer.usgs.gov/.

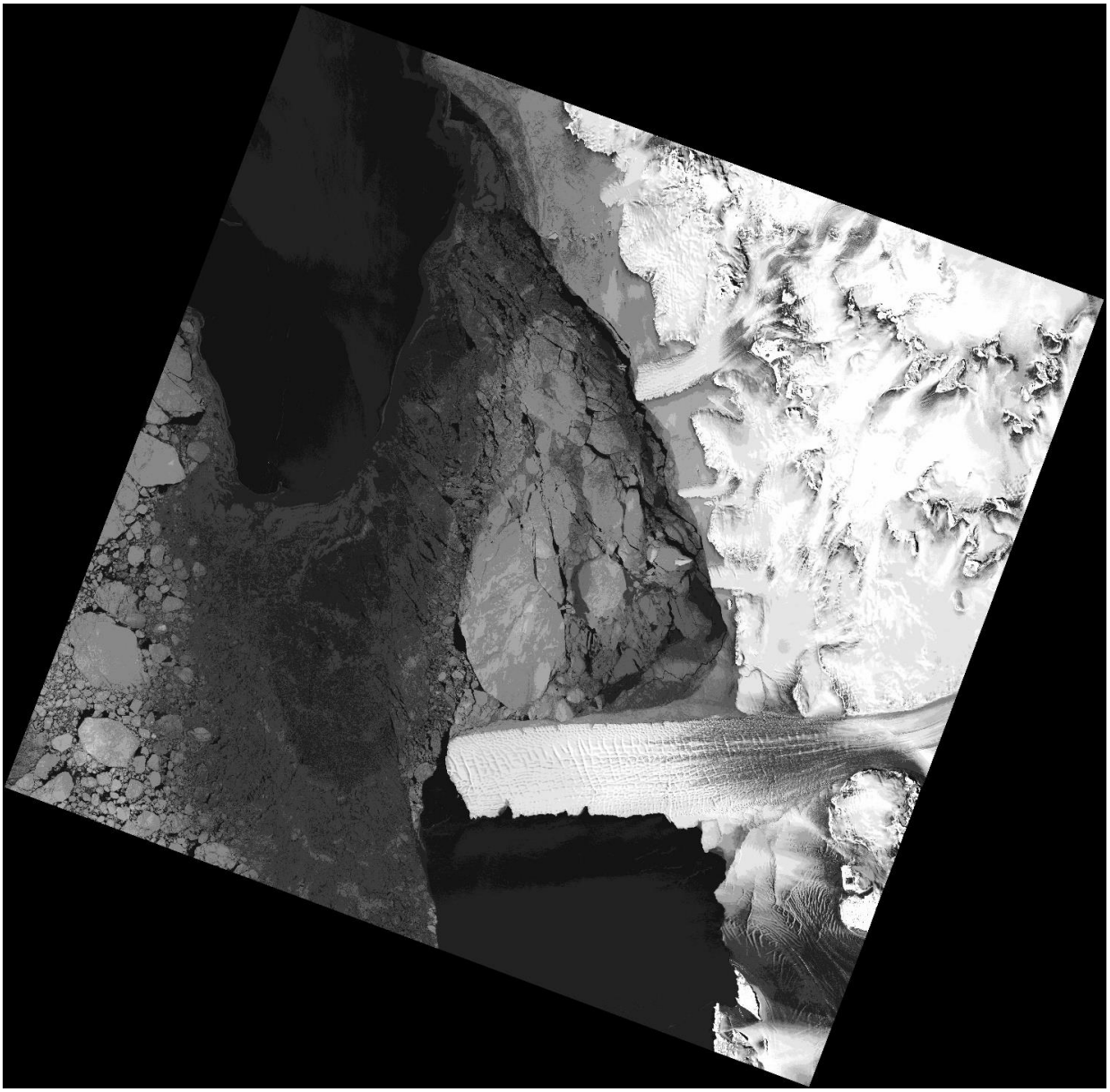

Figure 14. Single band (band 7 of Landsat-8) representation of the Drygalski ice tongue (lower-right part). Source: http://earthexplorer.usgs.gov/.

Acknowledgements

Even if the paper was devised together by the authors, M. Fea wrote paragraph 1 and supported paragraphs 3.1, 4.1, 5.1, 6.1, 7.1, 8.1; U. Minora and C. Smiraglia wrote paragraphs 3, 3.1, 4, 4.1, 5, 5.1, 6, 6.1, 7, 7.1, 8, 8.1; C. Pesaresi wrote paragraph 2.

References

1. Aðalgeirsdóttir G., Echelmeyer K.A. and Harrison W.D., "Elevation and volume changes on the Harding Icefield, Alaska", *Journal of Glaciology*, 44, 148, 1998, pp. 570-582.
2. Adhikary S., Nakawo M., Seko K. and Shakya B., "Dust influence on the melting process of glacier ice: Experimental results from Lirung Glacier, Nepal Himalayas", *IAHS Publ.*, 264, 2000, pp. 43-52.

3. Albright T.P., Painter T.H., Roberts D.A., Shi J.C., Dozier J. and Fielding E., "Classification of surface types using SIR-C/X-SAR, Mount Everest Area, Tibet", *Journal of Geophysical Research - B: Solid Earth and Planets*, 1998, pp. 25823-25837.
4. Arora M., "Outlet glacier", in Singh V.P., Singh P. and Haritashya (Eds.), *Encyclopedia of Snow, Ice and Glaciers*, Dordrecht, 2011, p. 799.
5. Bayr J.J., Hall D.K. and Kovalick W.M., "Observations on glaciers in the eastern Austrian Alps using satellite data", *International Journal of Remote* Sensing, 15, 9, 1994, pp. 1733-1742.
6. Berthier E., Arnaud Y., Baratoux D., Vincent C. and Rémy F., "Recent rapid thinning of the 'Mer de Glace' glacier derived from satellite optical images", *Geophysical Research Letters*, 31, 2004, pp. 1-4.
7. Berthier E., Arnaud Y., Rajesh K., Sarfaraz A., Wagnon P. and Chevallier P., "Remote sensing estimates of glacier mass balances in the Himachal Pradesh (Western Himalaya, India)", *Remote Sensing of Environment*, 108, 3, 2007, pp. 327-338.
8. Bolch T. and Kamp U., "Glacier Mapping in High Mountains Using DEMs, Landsat and ASTER Data", *8th International Symposium on High Moutain Remote Sensing Cartography, Grazer Schriften der Geographie und Raumforschung*, 41, 2006, pp. 37-48.
9. Bolch T., Menounos B. and Wheate R., "Landsat-based Inventory of Glaciers in Western Canada, 1985-2005", *Remote Sensing of Environment*, 114, 2010, pp. 127-137.
10. Bolch T. et al., "The State and Fate of Himalayan Glaciers", *Science*, 336, 6079, 2012, pp. 310-314.
11. Brock B.W., Mihalcea C., Kirkbride M., Diolaiuti G., Cutler M.E.J. and Smiraglia C., "Meteorology and surface energy fluxes in the 2005-2007 ablation seasons at Miage debris-covered glacier, Mont Blanc Massif, Italian Alps", *Journal of Geophysical Research*, 115, 2010, doi:10.1029/2009JD013224.
12. Citterio M., Diolaiuti G., Smiraglia C., D'Agata C., Carnielli T., Stella G. and Siletto G.B., "The recent fluctuations of Italian glaciers", *Geografiska Annaler*, 89, A3, 2007, pp. 164-182.
13. Cullen N.J., Mölg T., Kaser G., Hussein K., Steffen K. and Hardy D.R., "Kilimanjaro Glaciers: Recent areal extent from satellite data and new interpretation of observed 20th century retreat rates", *Geophysical Research Letter*, 33, 2006, doi:10.1029/2006GL027084.
14. Cullen N.J., Sirguey P., Mölg T., Kaser G., Winkler M. and Fitzsimons S.J., "A century of ice retreat on Kilimanjaro: The mapping reloaded", *The Cryosphere Discussion*, 6, 2012, pp. 4233-4265.
15. De Vecchis G. and Pesaresi C., *Dal banco al satellite. Fare geografia con le nuove tecnologie*, Rome, Carocci, 2011.
16. Deline P., "Change in surface debris cover on Mont Blanc massif glaciers after the 'Little Ice Age' termination", *The Holocene*, 2005, pp. 302-309.
17. Della Ventura A., Rabagliati R., Rampini A. and Serandrei Barbero R., "An application of ISIID: Remote Sensing Observation of Glaciers", *Second Conference on Images Analysis and Processing*, 1982, pp. 320-324.
18. Della Ventura A., Rabagliati R., Rampini A. and Serandrei Barbero R., "Remote-sensing observation of glaciers towards their monitoring", *Seventeeth International Symposium on Remote Sensing of Environment*, 1983, pp. 723-733.
19. Della Ventura A., Rabagliati R., Rampini A. and Serandrei Barbero R., "Controllo delle fluttuazioni dei ghiacciai alpini mediante telerilevamento da satellite", *Geografia Fisica e Dinamica del Quaternario*, 8, 1985, pp. 150-155.
20. Diolaiuti G., Kirkbride M.P., Smiraglia C., Benn D.I., D'Agata C. and Nicholson L., "Calving processes and lake evolution at Miage glacier, Mont Blanc, Italian Alps", *Annals of Glaciology*, 40, 2005, pp. 207-214.
21. Diolaiuti G., Bocchiola D., Vagliasindi M., D'Agata C. and Smiraglia C., "The 1975-2005 glacier changes in Aosta Valley (Italy) and the relations with climate evolution", *Progress in Physical Geography*, 6, 2012a, pp. 764-785.
22. Diolaiuti G., Bocchiola D., D'Agata C. and Smiraglia C., "Evidence of climate change impact upon glaciers' recession within the Italian Alps: the case of Lombardy glaciers",

Theoretical and Applied Climatology, 109, 2012b, pp. 429-445.
23. Dozier J., "Snow reflectance from Landsat-4 Thematic Mapper", *IEEE Transactions on Geoscience and Remote Sensing*, 1984, pp. 323-328.
24. Farinotti D., Huss M., Bauder A. and Funk M., "An estimate of the glacier ice volume in the Swiss Alps", *Global and Planetary Change*, 68, 2009, pp. 225-231.
25. Fea M., Giacomelli L., Pesaresi C. and Scandone R., "Remote sensing and interdisciplinary approach for studying volcano environment and activity", *Journal of Research and Didactics in Geography (J-READING)*, 1, 2, 2013, pp. 151-182.
26. Frey H., Huggel C., Paul F. and Haeberli W., "Automated detection of glacier lakes based on remote sensing in view of assessing associated hazard potentials", *Grazer Schriften der Geographie und Raumforschung*, 45, 2010, pp. 261-272.
27. Frezzotti M. and Mabin M.C.G., "20th century behaviour of Drygalski Ice Tongue, Ross Sea, Antarctica", *Annals of Glaciology*, 20, 1994, pp. 397-400.
28. Frezzotti M., Tabacco I.E. and Zirizzotti A., "Ice Discharge of eastern Dome C drainage area, Antarctica, determined from airborne radar survey and satellite image analysis", *Journal of Glaciology*, 46, 2000, pp. 253-273.
29. Gardelle J., Berthier E. and Arnaud Y., "Slight mass gain of Karakoram glaciers in the early twenty-first century", *Nature Geoscience*, 5, 2012, pp. 322-325.
30. Hall D.K., Riggs G.A. and Salomonson V.V., "Development of methods for mapping global snow cover using moderate resolution imaging spectroradiometer data", *Remote Sensing of Environment*, 54, 1995, pp. 127-140.
31. Hall D.K., Giffen B.A. and Chien J.Y.L., "Changes in the Harding Icefield and the Grewingk-Yalik Glacier Complex", *62nd Eastern Snow Conference*, Waterloo, ON, Canada, 2005, pp. 29-40.
32. Haq M.A., Jain K. and Menon K.P.R., "Change Monitoring of Gangotri Glacier using Remote Sensing", *International Journal of Soft Computing and Engineering (IJSCE)*, 1, 6, 2012, pp. 259-261.
33. Hardy D.R., "Kilimanjaro", in Singh V.P., Singh P. and Haritashya (Eds.), *Encyclopedia of Snow, Ice and Glaciers*, Dordrecht, 2011, pp. 672-679.
34. Hastenrath S., "Diagnosing the decaying glaciers of equatorial East Africa", *Meteorologische Zeitschrift*, 15, 2006, pp. 265-271.
35. Hubbard A. et al., "Glacier mass-balance determination by remote sensing and high-resolution modelling", *Journal of Glaciology*, 46, 154, 2000, pp. 491-498.
36. Huggel C., Kääb A., Haeberli W., Teysseire P. and Paul F., "Remote sensing based assessment of hazards from glacier lake outbursts: a case study in the Swiss Alps", *Canadian Geotechnical Journal*, 39, 2002, pp. 316-330.
37. Jiskoot H., "Glacier surging", in Singh V.P., Singh P. and Haritashya (Eds.), *Encyclopedia of Snow, Ice and Glaciers*, Dordrecht, 2011, pp. 415-428.
38. Jouvet G., Huss M., Funk M. and Blatters H., "Modelling the retreat of Grosser Aletschgletscher, Switzerland, in a changing climate", *Journal of Glaciology*, 57, 2011, pp. 1033-1045.
39. Kääb A., "Photogrammetric Reconstruction of Glacier Mass-Balance using a Kinematic Ice-flow Model. A 20-year Time-Series on Grubengletscher, Swiss Alps", *Annals of Glaciology*, 31, 2001, pp. 45-52.
40. Kääb A., Paul F., Maisch M., Hoelzle M. and Haeberli W., "The new remote sensing derived Swiss glacier inventory: II. First results", *Annals of Glaciology*, 34, 2002, pp. 362-366.
41. Kääb A. et al., "Remote sensing of glacier and permafrost-related hazards in high mountains: an overview", *Natural Hazards and Earth System Science*, 5, 2005, pp. 527-554.
42. Kaser G., Hardy D.R., Mölg T., Bradley R.S. and Hyera T.M., "Modern glacier retreat on Kilimanjaro as evidence of climate change: observations and facts", *International Journal of Climatology*, 24, 2004, pp. 329-339.
43. Kaufmann V., "The evolution of rock glacier monitoring using terrestrial photogrammetry: the example of Äusseres Hochebenkar rock glacier (Austria)", *Austrian Journal of Earth*

Sciences, 105, 2, 2012, pp. 63-77.
44. Kirkbride M., "Debris-covered glaciers", in Singh V.P., Singh P. and Haritashya (Eds.), *Encyclopedia of Snow, Ice and Glaciers*, Dordrecht, 2011, pp. 190-192.
45. Knoll C. and Kerschner H., "A glacier inventory for South Tyrol, Italy, based on airborne laser-scanner data", *Annals of Glaciology*, 50, 53, 2009, pp. 46-52.
46. Kulkarni A.V., Bahuguna I.M., Rathore B.P., Singh S.K., Randhawa S.S., Sood R.K. and Dhar S., "Glacial retreat in Himalaya using Indian Remote Sensing satellite data", *Current Science*, 92, 1, 2007, pp. 69-74.
47. Malinverni E.S., Croci C. and Sgroi F., "Glacier Monitoring by Remote Sensing and GIS Techniques in Open Source Environment", *EARSeL eProceedings*, 7, 2, 2008, pp. 120-132.
48. Masetti M., Diolaiuti G., D'Agata C. and Smiraglia C., "Hydrological characterization of an ice-contact lake: Miage Lake (Monte Bianco, Italy)", *Water Resources and Management*, 24, 2009, pp. 1677-1696.
49. Mattson L.E., Gardner J.S. and Young G.J., "Ablation on debris-covered glaciers: an example from the Rakhiot Glacier, Punjab, Himalaya", *IAHS Publ.*, 218, 1993, pp. 289-296.
50. Mihalcea C., Mayer C., Diolaiuti G., D'Agata C., Smiraglia C. and Tartari G., "Ice ablation and meteorological conditions on the debris covered area of Baltoro Glacier (Karakoram, Pakistan)", *Annals of Glaciology*, 43, 2006, pp. 292-300.
51. Mihalcea C., Brock B.W., Diolaiuti G., D'Agata C., Citterio M., Kirkbride M.P., Cutler M.E.J. and Smiraglia C., "Using ASTER satellite and ground-based surface temperature measurements to derive supraglacial debris cover and thickness patterns on Miage Glacier (Mont Blanc Massif, Italy)", *Cold Regions Science and Technology*, 52, 2008, pp. 341-354.
52. Minora U., Bocchiola D., D'Agata C., Maragno D., Mayer C., Lambrecht A., Mosconi B., Vuillermoz E., Senese A., Compostella C., Smiraglia C. and Diolaiuti G., "2001-2010 glacier changes in the Central Karakoram National Park: a contribution to evaluate the magnitude and rate of the 'Karakoram anomaly'", *The Cryosphere Discussion*, 7, 2013, pp. 2891-2941.
53. Mölg T., Hardy D.R. and Kaser G., "Solar-radiation-maintained glacier recession on Kilimanjaro drawn from combined ice-radiation geometry modeling", *Journal of Geophysical Research*, 108, 2003, p. 4731.
54. Mölg T., Cullen N.J., Hardy D.R, Winkler M. and Kaser G., "Quantifying Climate Change in the Tropical Midtroposphere over East Africa from Glacier Shrinkage on Kilimanjaro", *Journal of Climate*, 22, 2009, pp. 4162-4181.
55. Moore G., "Satellite remote sensing of water turbidity", *Hydrological Sciences-Bulletin-des Sciences Hydrologiques*, 25, 4, 1980, pp. 407-421.
56. Morgan V.I., Jacka T.H., Ackerman G.J. and Clarke A.L., "Outlet glaciers and mass-budget studies in Enderby, Kemo and Mac. Robertson lands, Antarctica", *Annals of Glaciology*, 3, 1982, pp. 204-210.
57. Nakawo M. and Rana B., "Estimate of ablation rate of glacier ice under a supraglacial debris layer", *Geografiska Annaler*, 81A, 4, 1999, pp. 695-701.
58. Negi H.S., Thakur N.K., Ganju A. and Snehmani, "Monitoring of Gangotri glacier using remote sensing and ground observations", *Journal of Earth System Science*, 121, 4, 2012, pp. 855-866.
59. Nuth C., Kohler J., Aas H.F., Brandt O. and Hagen J.O., "Glacier geometry and elevation changes on Svalbard (1936–90): a baseline dataset", *Annals of Glaciology*, 46, 2007, pp. 1-11.
60. Osmaston H., "Glaciers, glaciations and equilibrium line altitudes on Kilimanjaro", in Mahaney W.C. (Ed.), *Quarternary and environmental research on East African mountains*, Rotterdam, Balkema, 1989, pp. 7-30.
61. Paul F., "Changes in glacier area in Tyrol, Austria, between 1969 and 1992 derived from Landsat 5 Thematic Mapper and Austrian Glacier Inventory data", *International Journal of Remote Sensing*, 23, 4, 2002, pp. 787-799.
62. Paul F., Kääb A., Maisch M., Kellenberger T. and Haeberli W., "The new remote-sensing-derived Swiss glacier inventory: I. Methods", *Annals of Glaciology*, 34, 2002, pp. 355-361.

63. Paul F., Kääb A. and Haeberli W., "Recent glacier changes in the Alps observed by satellite: Consequences for future monitoring strategies", *Global and Planetary Change*, 56, 2007, pp. 111-122.
64. Paul F. et al., "On the accuracy of glacier outlines derived from remote-sensing data", *Annals of Glaciology*, 54, 63, 2013, pp. 171-182.
65. Rabagliati R. and Serandrei Barbero R., "Possibilità d'impiego del remote sensing da satellite per il controllo annuale dei ghiacciai", *Geografia Fisica e Dinamica del Quaternario*, 2, 1979, pp. 35-40.
66. Racoviteanu A.E., Williams M.W. and Barry R.G., "Optical Remote Sensing of Glacier Characteristics: A Review with Focus on the Himalaya", *Sensors*, 8, 2008, pp. 3355-3383.
67. Scherler D., Bookhagen B. and Strecker M., "Spatially variable response of Himalayan glaciers to climate change affected by debris cover", *Nature Geoscience*, 4, 2011, pp. 156-159.
68. Shi J.C. and Dozier J., "Mapping seasonal snow with SIR-C/X-SAR in mountainous areas", *Remote Sensing of Environment*, 59, 2, 1997, pp. 294-307.
69. Smiraglia C. and Diolaiuti G., "Epiglacial Morphology", in Singh V.P., Singh P. and Haritashya (Eds.), *Encyclopedia of Snow, Ice and Glaciers*, Dordrecht, 2011, pp. 262-268.
70. Stringer W.J. and Groves J.E., "Location and Areal Extent of Polynyas in the Bering and Chukchi Seas", *Arctic*, 44, 1991, pp. 164-171.
71. Tabacco I.E., Bianchi C., Chiappino M., Zirizzotti A. and Zuccheretti E., "Analysis of bottom morphology of the David Glacier-Drigalski Ice Tongue, East Antartica", *Annals of Glaciology*, 30, 2000, pp. 47-51.
72. Villa F., Sironi S., DeAmicis M., Maggi V., Zucca F. and Tamburini A., "Integration of Different Kind of Remote Sensing Data as a Tool for Quantitative Analysis of Glacier Evolution", *9th International Symposium on High Mountain Remote Sensing Cartography, Grazer Schriften der Geographie und Raumforschung*, 43, 2007, pp. 103-108.
73. WGMS (compiled by Zemp M., Frey H., Gärtner-Roer I., Nussbaumer S.U., Hoelzle M., Paul F. and Haeberli W.), *Fluctuations of Glaciers 2005-2010*, vol. X, Zurich, Switzerland, ICSU(WDS)/IUGG(IACS)/UNEP/UNESCO/WMO, World Glacier Monitoring Service, 2012.
74. Williams R.S. and Ferrigno J.G. (Eds.), *Satellite Image Atlas of Glaciers of the World. State of the Earth's Cryosphere at the Beginning of the 21st Century: Glaciers, Global Snow Cover, Floating Ice, and Permafrost and Periglacial Environments*, U.S. Geological Survey, Professional Paper 1386–A, Washington, United States Government Printing Office, 2012.
75. Wuite J., Jezek K.C., Wu X., Farness K. and Carande R., "The velocity field and flow regime of David Glacier and Drygalski Ice Tongue, Antarctica", *Polar Geography*, 9, 2009, pp. 111-127.

